Kaolin Clay Reinforced with a Granular Column Containing Crushed Waste Glass or Traditional Construction Sands

1. Danish Kazmi (corresponding author)

Affiliation
Geotechnical Engineering Centre, School of Civil Engineering, The University of Queensland, Brisbane, QLD 4072, Australia
Positions
Research Scholar
Email address
d.kazmi@uq.net.au

2. Mehdi Serati

Affiliation
Geotechnical Engineering Centre, School of Civil Engineering, The University of Queensland, Brisbane, QLD 4072, Australia
Position
Lecturer
Deputy Manager, Large Open Pit Project (www.lopproject.com)
Email address
m.serati@uq.edu.au

3. David J. Williams

Affiliation
Geotechnical Engineering Centre, School of Civil Engineering, The University of Queensland, Brisbane, QLD 4072, Australia
Position
Professor of Geotechnical Engineering
Director, Geotechnical Engineering Centre
Manager, Large Open Pit Project (www.lopproject.com)
MWT 2020 Conference Chair
Email address
d.williams@uq.edu.au

4. Sebastian Quintero Olaya

Affiliation
Geotechnical Engineering Centre, School of Civil Engineering, The University of Queensland, Brisbane, QLD 4072, Australia
Position
Senior Research Officer
Email address
s.quintero@uq.edu.au

5. Sadaf Qasim

Affiliation
Department of Civil Engineering, NED University of Engineering and Technology, Karachi, 75270, Pakistan
Position
Associate Professor
Email address
erum@neduet.edu.pk

6. Yi Pik Cheng

Affiliation
Department of Civil, Environmental and Geomatic Engineering, University College London, London, WC1E 6BT, United Kingdom
Position
Senior Lecturer
Email address
yi.cheng@ucl.ac.uk

7. J. Antonio H. Carraro

Affiliation
Department of Civil and Environmental Engineering, Imperial College London, London, SW7 2AZ, United Kingdom
Position
Senior Lecturer in Experimental Geotechnical Engineering
Email address
antonio.carraro@imperial.ac.uk

Abstract

Installation of granular columns is a cost-effective and versatile *in situ* technique to improve the shear strength, settlement, and drainage behaviour of weak soils. It involves backfilling vertical boreholes in the ground with granular materials stiffer than the native soil, such as stone or compacted sand. However, the massive use and overexploitation of sand and natural aggregates have depleted their reserves in recent decades, causing damage to the environment, creating sand shortages and skyrocketing their price. Hence, it is essential to develop a sustainable alternative to natural aggregates to construct granular columns. The ever-increasing stockpiles of waste glass could be a potential replacement for natural sand in several geotechnical construction applications, noting that both materials have a similar chemical composition. Using crushed waste glass (CWG) as an alternative to traditional natural and manufactured (quarried) sands in granular columns could offer a multi-pronged benefit by recycling non-biodegradable waste (glass) and by conserving a depleting natural resource (sand). Using a large direct shear (LDS) machine, this study investigated the shear strength behaviour of kaolin (to represent a typical weak soil) reinforced with a central granular column. Three different materials were separately used to backfill the column, including natural sand (NS), manufactured sand (MS) and CWG. The results revealed that the geocomposites containing the CWG

column have the highest peak friction angle and relatively greater shear strength under high normal stresses, favouring the potential use of CWG as a green alternative to traditional sands in backfilling granular columns, ultimately supporting resource conservation, waste recycling and the paradigm shift towards a circular economy.

Keywords

Granular columns; natural aggregates; crushed waste glass; large direct shear machine; shear strength; geocomposites; circular economy

Introduction

As cities grow, the need to develop low-lying and coastal areas inevitably increase. Low-lying lands are often overlain by soft or loose soils, which are highly compressible and typically marked by low shear strength Malarvizhi (2007), requiring ground improvement before the foundations for new infrastructure could be constructed (Alfaro et al., 1994). Similar challenges are sometimes encountered for inland sand deposits due to water fluctuations in the soil caused by weather changes (Sivakumar et al., 2014). Poor ground properties could be detrimental to infrastructures. For example, the annual damage caused by expansive soils to civil engineering structures is around $1,000 million in the USA, $150 million in the UK and at least $4 million in South Africa (Gourley et al., 1993). The growing land prices and the limited availability of suitable construction sites encourage the need for ground improvement (Babu et al., 2013). Several ground improvement techniques have been developed to improve the geotechnical characteristics of weak *in situ* soils, such as bearing capacity and settlement (Andreou et al., 2008).

Of all the ground improvement techniques available, granular columns, also known as sand or stone columns, granular piles or granular inclusions, are considered one of the most cost-effective and versatile *in situ* ground improvement techniques whose concept was first applied in France in 1830 (Babu et al., 2013). In this technique, vertical boreholes are formed in the soil that are filled upwards with compacted granular backfill such as sand or stone (Castro, 2017). They can be used to improve several types of soil, from soft clays to loose sands, making them one of the preferred ground improvement techniques (Abhishek et al., 2016). They also serve as vertical drains and dissipate excess pore water pressure due to loading by providing a shorter drainage path of higher permeability, thereby increasing the consolidation rate and reducing the time required for post-construction ultimate settlements (Abhishek et al., 2016; McCabe et al., 2007). Another key benefit of granular columns is the densification of the *in situ* soil surrounding the columns, which enhances the compaction characteristics of the *in situ* soil (Ranjan, 1989). Moreover, granular columns could

112 effectively mitigate potential liquefaction or softening of susceptible soils through reinforcement,
113 drainage and densification (Abhishek et al., 2016).

114 According to Sivakumar et al. (2004), a granular column develops end-bearing pressure and shear
115 stresses when loaded vertically, causing the column to expand laterally and mobilise lateral support
116 from the surrounding soil. This increase in lateral stress consolidates the surrounding clay once the
117 excess pore water pressure dissipates and causes further bulging in the column. This process goes on
118 until equilibrium is achieved at the boundary between the column and the surrounding soil. As a result,
119 the column and the surrounding soil behave as a composite with a higher stiffness than the original
120 soil (Mohapatra et al., 2014). The net result is that the entire site where the columns are installed then
121 displays higher strength, improved bearing capacity and stiffness. Technically, granular columns
122 largely obtain their load capacity from the confinement provided by the surrounding soil by mobilising
123 passive earth pressure (Babu et al., 2013). However, for very soft clays with very low undrained shear
124 strength (<15 kN/m^2), such soils provide insufficient lateral confinement causing the columns to
125 undergo excessive bulging and settlements that reduce the load-carrying capacity and the
126 effectiveness of granular columns (Murugesan and Rajagopal, 2007).

127 Granular columns are mostly installed using the vibro-flotation technique, whose typical installation
128 process is schematically shown in Figure 1. A vibroflot (or vibrating poker) is inserted into the ground
129 to create a vertical hole that is incrementally filled with compacted sand or stone (Ranjan, 1989).
130 Vibro-replacement is generally used for clayey soils (Priebe, 1995). Moreover, granular columns are
131 environment-friendly (Hanna et al., 2013; Mehrannia et al., 2018). They release relatively lower
132 greenhouse gas emissions and consume relatively less fuel during their installation (Chawla et al.,
133 2010).

134 Theoretically, the unit cell model is mostly used to analyse granular columns (Castro, 2017). It consists
135 of a single column and its corresponding tributary area transformed into an equivalent circle (influence
136 zone) with the same cross-sectional area (Ng and Tan, 2015). The diameter of a unit cell is equal to d_e

= 1.05 – 1.13s for triangular and square grids, respectively, where s is the centre-to-centre spacing between columns (Castro, 2017). Several parameters influence the behaviour of soil reinforced with granular columns, including the area replacement ratio, length and diameter of the column, material properties of the column backfill, spacing between the columns and the installation pattern of the columns (Babu et al., 2013; Bergado et al., 1990; Poorooshasb and Meyerhof, 1997; Priebe, 1995).

Literature review

Several studies have examined the geotechnical performance of soil treated with granular columns. Some of these studies compared the shear resistance and load-settlement response of ordinary and geotextile-encased columns (e.g. Mohapatra et al. 2014, Malarvizhi 2007); however, they are not the focus of this study.

Canakci et al. (2017) investigated the shear strength (direct shear) and compressibility (oedometer) performance of fibrous peat soil (liquid limit of 119%) reinforced with a sand column. Rounded poorly-graded sand, passing a 2-mm sieve and retained on a 1-mm sieve, was used to construct the column at three different area replacement ratios (11.5%, 25% and 49%). Their study found that installing a sand column improved the peat's compressibility and shear strength behaviour, with compressibility characteristics improving with increase in the area replacement ratio.

Similarly, Najjar et al. (2010) examined the mechanical behaviour of normally consolidated clay (kaolin) reinforced with encased and non-encased sand columns. The sand columns comprised poorly graded Ottawa sand with a friction angle of 33^{o} and were installed at a relative density of nearly 44%. A total of 32 isotropically consolidated undrained (CU) triaxial tests was conducted on reinforced specimens with area replacement ratios of 7.9% and 17.8%. The study found that the sand columns considerably reduced the generation of excess pore water pressure during undrained loading. It was also noted that increasing the area replacement ratio from 7.9% to 17.5% considerably increased the undrained shear strength of kaolin reinforced with fully-penetrating non-encased sand columns.

Aslani et al. (2019) investigated the shear strength behaviour of clay reinforced with granular columns containing gravel (D_{50} = 0.52 mm) or stone (D_{50} = 4.2 mm). Using a large direct shear machine with an area of 305 mm x 305 mm and depth of 152.4 mm, tests were performed on geocomposites containing three different area replacement ratios (13.3%, 17.7% and 24%), different installation patterns (single, square and triangular) and different normal stresses (35 kPa, 55 kPa and 75 kPa). Their study concluded that the shear strength of the geocomposites increased with increasing area replacement ratio in all granular column installation patterns. The study also observed that installing a granular column increased the stiffness of reinforced clay compared to the unreinforced clay.

Barmade et al. (2021) investigated the load-settlement behaviour of expansive soil reinforced with stone columns with diameters of 40 mm, 60 mm and 80 mm. Their study concluded that installing stone columns improved the bearing pressure of the reinforced soil, while the columns also increased the drainage of the soil. Hence, the benefits of installing granular columns in weak soils are well-established in the literature, as discussed in the reviewed studies (Babu et al., 2013; Manohar and Patel, 2021; Mokhtari and Kalantari, 2012; Najjar, 2013).

Why should crushed waste glass be considered for use as an alternative to traditional construction sands?

Natural aggregates are fundamentally used to create granular columns. However, due to the continued use and heavy reliance of the construction industry, the aggregates (sand and stone) suitable for construction are rapidly depleting globally (Holmstrom and Swan, 1999; Kazmi et al., 2020; Kazmi et al., 2019). Studies show that sand and gravel are being mined at a rate greater than their renewal (Bendixen et al., 2019). As a result, the global demand for natural sand and gravel has skyrocketed to almost 50 billion tonnes per year, averaging 18 kg/person/day (UNEP, 2019). Today many countries in the world face an approaching risk of a shortage of aggregates (Langer et al., 2004). Simultaneously, the mining of aggregates and associated activities typically releases a carbon footprint that is harmful to the environment (Bravo et al., 2015; Kazmi et al., 2020). Thus, there is a growing

need to develop a sustainable replacement for natural and manufactured (quarried) sands in construction, including geotechnical applications (Kazmi et al., 2020). The ever-increasing volumes of waste glass could provide such an alternative (Kazmi et al., 2021). Nearly 10, 15 and 1 million tons of waste glass are stockpiled every year in United States, European Union and Australia, respectively, creating a challenge for their safe and sustainable disposal (Saberian et al., 2019). According to Kazmi et al. (2019), given the growing quantities of waste glass and diminishing reserves of natural sand, the use of waste glass as a substitute for natural and manufactured (quarried) sand could provide two-pronged benefits of cost-effectiveness and environmental sustainability. In cities, waste glass is typically produced in greater volumes, and quarries are often distant from project sites. Using crushed waste glass (CWG) as an alternative geomaterial could be economical due to low material cost, reduced travel distance and shorter transportation time. Simultaneously, as waste glass is non-biodegradable, such utlisation of CWG could promote waste recycling, decrease burden on landfills, reduce greenhouse gas emissions and conserve natural raw materials, ultimately all leading towards a circular economy.

Common safety concerns associated with the use of crushed waste glass

Generally, a common safety concern associated with using CWG is the risk of skin cut due to sharp edges of glass particles (Ali, 2012). However, practical experience suggests that glass particles finer than 19 mm poses no greater cut or penetration risk than an ordinary fractured natural aggregate (Ali, 2012). Another common concern about the use of glass is the risk of contracting silicosis; a respiratory disease caused when crystalline silica is inhaled. However, during the glass manufacturing process, the crystalline silica is largely turned into amorphous silica, which does not primarily lead to silicosis (Clean Washington Center, 1996). Moreover, previous studies show that CWG could be a potential replacement for natural sand in several geotechnical construction applications (Wartman et al., 2004; Disfani et al., 2011; Arulrajah et al., 2013). Kazmi et al. (2021) compared the geotechnical, mineralogical and morphological behaviour of CWG with those of natural sand (NS) and manufactured sand (MS). Their study concluded that CWG has geotechnical behaviour similar to traditional

212 construction sands and could potentially be utilised as an alternative smart geomaterial in several
213 geotechnical construction applications (Kazmi et al., 2021).

214 *Use of alternative geomaterials in granular columns*

215 Granular columns offer an ideal opportunity to utilise recycled aggregates as column backfill (Egan
216 and Slocombe, 2010). However, limited research is done on using alternative materials (waste) to
217 backfill granular columns (Ayothiraman and Soumya, 2015). A few researchers observed some
218 favourable behaviour of granular columns backfilled with different alternative materials, including
219 tyre chips, recycled crushed brick, recycled crushed concrete, recycled railway track ballast,
220 incinerator bottom ash aggregate (IBAA) and construction and demolition waste (Alnunu and
221 Nalbantoglu, 2019; Amini, 2016; Ayothiraman and Soumya, 2015; Kumar and Sadana, 2012; Serridge,
222 2004; Serridge and Sarsby, 2009; Shahverdi and Haddad, 2020). However, despite enormous potential,
223 no detailed study has been found to date investigating the use of CWG as a backfill in granular
224 columns.

225 To fill this research gap, this study investigates the shear strength behaviour of geocomposites (soil
226 reinforced with a granular column) with a granular column containing CWG and installed in the centre
227 of a weak clayey soil (kaolin). Several reasons led to the selection of kaolin as the weak soil in this
228 study. Firstly, kaolin has relatively low shear strength and often requires some form of treatment or
229 reinforcement to support applied loads. Also, kaolin is readily available commercially, and its
230 information database is extensive due to the large number of studies involving its use (Mishra et al.,
231 2018a; Mishra et al., 2018b; Mishra et al., 2020; Rossato et al., 1992). The novelty of this paper is that
232 it compares the shear strength behaviour of geocomposites containing a CWG column with those
233 containing a column made up of NS or MS, which are traditionally used in sand column construction
234 (Zukri and Nazir, 2018).

235

236

Methodology

In this study, a series of large direct shear tests (LDST) on cubical specimens with length, width and height equal to 150 mm were performed to study the shear strength behaviour of geocomposites. Each geocomposite comprised of a cubical kaolin clay specimen (bed material) with a vertical granular column installed in its centre. Distinct geocomposites were prepared using columns containing three different types of column backfill. The LDS tests were also performed on kaolin only specimens as a reference to compare its shear strength behaviour with that of column-kaolin geocomposites. Three different materials were separately used to backfill the granular column, including NS, MS or CWG.

Table 1 shows the results of the mineralogical analysis performed on NS, MS and CWG using X-ray fluorescence (XRF) spectroscopy, showing that silica (SiO_2) is the primary mineral in all three materials. Table 2 presents the geotechnical characterisation results of all the test materials, as reported by Kazmi et al. (2021) and Xu et al. (2018), showing that NS and CWG are uniformly graded materials with median particle sizes of 0.29 mm and 1.42 mm, respectively. The median particle size of NS is almost five times smaller than that of CWG. MS, however, is a well-graded sand with a median particle size of 1.55 mm. Figure 3 shows the gradation curves of the test materials.

The morphological analysis revealed that MS has the highest particle angularity, followed by CWG and NS. This implies that NS particles are relatively more rounded than MS and CWG particles. Figure 2 shows the optical microscopic images of NS, MS and CWG particles. Also, the permeability tests revealed that CWG has the highest permeability, followed by NS and MS. CWG has the lowest minimum dry density and the largest difference between maximum and minimum dry density values. The critical-state friction angle of CWG increased by almost 11%, from 29.1^o under dry conditions to 32.4^o under saturated conditions.

The kaolin used in this study is a highly plastic clay (CH) with a liquid limit and plasticity index of 90% and 55%, respectively. The percentage of material passing the #200 sieve (F_{200}) is 69% for the kaolin.

261 The advanced high-accuracy large direct shear test machine (LDSM), ADS-300, manufactured by Wille
262 Geotechnik in Germany, was used to test the shear strength of all the specimens. The machine is
263 equipped with four linear variable differential transducers (LVDTs) on four corners of the top-loading
264 cap, recording the average settlement value. The testing setup also features a computer with data
265 logging software to precisely record the measurements. The size of all the geocomposites tested was
266 150 mm x 150 mm x 150 mm. A key reason to use the LDSM is that it provides the ability to test
267 relatively large specimens alongside better control over specimen design parameters. This helps in
268 minimising the size effect and modelling the field conditions more accurately. The device also
269 monitors tilting through the four LVDTs, making tests more accurate. If the tilting exceeds 10% of the
270 specimen height, the machine stops automatically. The LDSM used is capable of testing the specimens
271 according to ASTM D3080-11 and BS 1377-7. Figure 4 shows the LDSM used.

272 The kaolin (Eckalite 1) used in this study is high-quality water washed china clay with controlled
273 particle size distribution and colour, manufactured under a quality system certified facility. For sample
274 preparation, the kaolin was mixed with water using a mechanical mixer and prepared at an average
275 water content, consistency index and liquidity index of 56%, 0.61 and 0.38, respectively. The
276 undrained shear strength (S_u), in kPa, of kaolin was estimated to be approximately 29.3 kPa using the
277 following correlation proposed by Wroth and Wood (1978):

278 $$S_u = 170 \times \exp(-4.6 \times LI) \quad (1)$$

279 where, LI is the liquidity index of the soil.

280 Afterwards, the prepared kaolin was thoroughly mixed and soaked for at least 24 hours in an airtight
281 container to ensure uniform water consistency. Necessary care was practised to prevent lumps from
282 being left in the prepared kaolin. The dry density of the kaolin bed was set constant to 10 kN/m^3 for
283 all the specimens. The kaolin bed was prepared by compacting the pre-weighted kaolin in three equal
284 layers spread and compacted evenly using a hand tamper to avoid any air entrapment between the
285 layers of kaolin. The thickness of each kaolin layer was maintained at 50 mm. Kaolin samples were

286 taken from the leftover of kaolin bed every time the specimen was prepared to determine the most
287 representative water content.

288 With a column penetration ratio (C_r), defined as the height of the column to the height of the
289 specimen, of 1.0, an end-bearing granular column was installed in the centre of the kaolin bed through
290 the replacement method. A thin-walled polyvinyl chloride (PVC) tube, with a thickness of 2.5 mm and
291 an external diameter of 68mm, was used to construct the granular column. The end-bearing column
292 was created because the increase in column length significantly improves the behaviour of reinforced
293 soil, mainly due to sufficient mobilisation of end-bearing capacity and skin resistance through an
294 increase in the peripheral area and overburden stress (Dash and Bora, 2013). An adequate gap was
295 maintained between the shear box and the boundaries of the granular column to avoid the boundary
296 effect during the test. The PVC tube was gradually pushed vertically and concentrically into the kaolin
297 bed until it reached the base of the shear box. A static force was applied to drive the PVC tube into
298 the kaolin to minimise the disturbance in the surrounding kaolin. After installing the PVC tube, the
299 kaolin within the tube was scooped out using a stainless steel spatula. All the geocomposites were
300 prepared at an area replacement ratio (A_r) of 16%. A_r is defined as the plan area of the column to the
301 plan area of the shear box. This A_r was selected to avoid the influence of the shear box boundary on
302 the results. The column's length to diameter (L/D) ratio was 2.2, ensuring that the column was within
303 its critical length. The pre-weighed quantity of oven-dried granular backfill was carefully charged into
304 the resulting hole using a funnel. The column backfill was compacted in three different layers using a
305 hand tamper to achieve a relative density (or density index) of 60%. This relative density was adopted
306 to ensure there was no lateral bulging of the column to avoid disturbance to the surrounding kaolin.
307 Another reason for choosing this relative density was to pick a value that correlates with the practical
308 conditions. The column backfill was compacted till both kaolin and column reached the same height.
309 Afterwards, the cylindrical PVC tube was gradually withdrawn from the kaolin bed by carefully pulling
310 it upwards. Samples were taken from the leftover of the prepared kaolin bed just before starting the
311 LDS test to perform the water content testing. The shearing plane was situated in the middle of the

312 sample (at 75 mm height). Overall, this procedure was found to give repeatable and uniform
313 specimens of good quality. The typical plan and cross-section of the geocomposite are shown in Figure
314 5a and 5b, respectively.

315 The single-stage (implying that a new specimen was prepared for test under each load) stress-
316 controlled LDS experiments were performed on the prepared kaolin only specimens and the
317 geocomposites. The geocomposites were tested separately under 12.5 kPa, 25 kPa, 50 kPa and 100
318 kPa normal stress, with the normal stress increasing at a load increment factor of 1.0. All the
319 geocomposites and kaolin only specimens were consolidated under each normal stress before
320 shearing them uniformly at a slow rate of 0.02 mm/min to allow the column to mobilise its drainage
321 capacity. The specimens were allowed to drain water and were not inundated during the test. The test
322 was stopped when the shear stress became constant, or the shear displacement reached 28 mm (18%
323 shear strain). The stress and displacement data were continuously recorded using the LVDT and
324 computerised data acquisition system. Altogether, sixteen LDS tests were performed. Figure 6a, 6b,
325 6c and 6d represents the top view of the kaolin specimen, the NS-kaolin, the MS-kaolin and the CWG-
326 kaolin geocomposite before the test, respectively.

327 **Experimental results**

328 The obtained results were used to develop the shear strength envelopes that were best-fitted using
329 the Coulomb failure criterion. The peak shear strength from each experiment was plotted against the
330 corresponding normal stress to develop the envelope. The shear strength of all the specimens was
331 found to increase with normal stress. The applied normal stresses and measured shear stresses were
332 corrected for reductions in the shear area during specimen shearing. The fitting parameters for each
333 envelope were determined in terms of the Nash-Sutcliffe model efficiency coefficient (NSE) and the
334 coefficient of determination (R^2). Given the criteria suggested by Chiew and McMahon (1993), the
335 goodness-of-fit of all shear strength envelopes given in this paper can be rated as “perfect” (NSE ≥
336 0.93). Table 3 shows the peak friction angle of the kaolin only specimens and the geocomposites.

Figure 7 shows the peak shear strength envelopes of the kaolin only specimens and the geocomposites.

The results show that the cohesion of kaolin only specimens is 1.7 kPa, whereas its friction angle is 14.0^{o}. Overall, installing a granular column increased the shear strength of the geocomposite, regardless of the type of column backfill used. The shear strength parameters of kaolin only specimens were considered as a reference for comparison.

The results of the NS-kaolin geocomposite showed that installing the NS column increased the friction angle from 14.0^{o} to 17.8^{o}, an increase of 27%, whereas the cohesion increased over two-fold from 1.7 kPa to 3.9 kPa. Compared to the kaolin only specimens, the increase in the friction angle of the NS-kaolin geocomposite appears largely due to the inclusion of the NS column, as the characterisation testing previously showed that NS has a peak friction angle of 36.9^{o} under dry conditions. It is postulated that the NS-kaolin geocomposite derives its cohesion (3.9 kPa) from two parts: the true cohesion of kaolin and the apparent cohesion of NS.

The results of the MS-kaolin geocomposite showed an increase in both the cohesion and friction angle. The friction angle of the MS-kaolin geocomposite increased to 17.7^{o}, an increase of 26%, which is similar to that of the NS-kaolin geocomposite. However, the MS column considerably increased the cohesion of the geocomposite to 5.4 kPa, an increase of over three-fold. Also, the peak shear strength of the MS-kaolin geocomposite was higher than that of the NS-kaolin geocomposite under all the applied normal stresses. The reason for the higher peak shear strength of the MS-kaolin geocomposite compared with that of the NS-kaolin geoomposite could be the more well-graded MS, its higher particle angularity and its larger median particle size.

The results of the CWG-kaolin geocomposite showed a two-fold increase in cohesion compared with kaolin alone, which is somewhat similar to that of the NS-kaolin geocomposite. Importantly, installing the CWG column showed the highest increase in friction angle, increasing from 14.0^{o} for kaolin alone to 20.7^{o}. The reason for the relatively higher friction angle of the CWG-kaolin geocomposite and lower

362 cohesion could be the higher Young's Modulus of the CWG particles. The Young's Modulus of CWG
363 particles is approximately 40 to 90 Gpa (Hsieh et al., 2009; University of Texas, 2019; Qi et al., 2012;
364 Karabulut et al., 2001; Engineering ToolBox, 2003), whereas that of sand and gravel particles generally
365 varies from 10 to 170 MPa (University of Texas, 2019; Schanz and Vermeer, 1998). The higher Young's
366 Modulus of CWG potentially attracts greater stress to the CWG column, leading to more stress being
367 taken by the CWG column than the surrounding kaolin. As a result, the granular characteristics of the
368 geocomposite become more dominant during shearing.

369 Figures 8a and 9a present the shear stress-horizontal displacement and horizontal-vertical
370 displacement behaviour of kaolin alone, respectively. Figures 8b, 8c and 8d present the shear stress-
371 horizontal displacement behaviour of NS-kaolin, MS-kaolin and CWG-kaolin geocomposites,
372 respectively. Similarly, Figures 9b, 9c and 9d present the horizontal-vertical displacement behaviour
373 of NS-kaolin, MS-kaolin and CWG-kaolin geocomposites, respectively. The shear stress-horizontal
374 displacement behaviour of the kaolin only specimens showed that the shear stress non-linearly
375 increased with an increase in shear displacement. The horizontal-vertical displacement behaviour of
376 the kaolin only specimens showed progressively higher vertical displacement with increasing normal
377 stress, with over 10 mm compression observed under 100 kPa normal stress. It was also noted that
378 the amount of vertical displacement during shearing under higher normal stress (100 kPa) was highest
379 in kaolin alone compared to all of the geocomposites.

380 The shear stress-horizontal displacement behaviour of the NS-kaolin geocomposite showed a clear
381 peak in shear stress under 100 kPa normal stress. The horizontal-vertical displacement behaviour of
382 the NS-kaolin geocomposite showed that the lowest and highest vertical displacement occurred under
383 100 kPa and 50 kPa normal stress, respectively. A sharp drop in vertical stress was also noted in the
384 NS-kaolin geocomposite at approximately 17 mm horizontal displacement under 12.5 kPa normal
385 stress. This drop in vertical displacement would have densified the specimen, leading to a slight
386 increase in shear stress. The MS-kaolin geocomposite showed two distinct rises and falls in shear stress
387 between 1-3 mm horizontal displacement under 50 kPa normal stress, possibly due to the dispersion

388 of microcracks or rearrangement of sand particles. Another potential reason for these sudden changes
389 could be that some sand particles at the column-kaolin interface started to penetrate the kaolin,
390 leading to a sudden drop in shear stress. When the smear zone was created, the shear stress restarted
391 to increase (Xu et al., 2018).

392 The horizontal-vertical displacement behaviour of the MS-kaolin geocomposite showed a drop in
393 vertical displacement between 12-13 mm and 20-21 mm horizontal displacement under 12.5 kPa
394 normal stress. This drop in vertical displacement would have densified the MS-kaolin geocomposite,
395 increasing the shear stress at these horizontal displacements, as for the NS-kaolin geocomposite. Also,
396 the shear stress-horizontal displacement behaviour of the CWG-kaolin geocomposite showed a
397 relatively higher increase in shear stress with increasing normal stress. A sharp rise and fall in shear
398 stress were also observed between 3-4 mm horizontal displacement under 50 kPa normal stress,
399 possibly due to localised strain-softening, which is somewhat comparable to the MS-kaolin
400 geocomposite results. Figure 9d shows a relatively smooth, non-linear and comparable horizontal-
401 vertical displacement behaviour under 12.5 kPa, 25 kPa and 100 kPa normal stress, with relatively
402 much higher vertical displacement under 50 kPa normal stress.

403 For all three geocomposites, the highest vertical displacement was observed under 50 kPa normal
404 stress, with the vertical displacement reducing under 100 kPa. The potential reason for this could be
405 greater stress concentration on the column under higher normal stresses, reducing the kaolin's
406 contribution to shear strength and allowing the column to dominate the system.

407 Figure 10 compares the maximum vertical displacement (compression) of all the specimens during
408 shearing with their corresponding applied normal stress. It can be seen that the significant reduction
409 in the maximum vertical displacement (less compression) occurs under the applied normal stress of
410 100kPa for all three geocomposites, potentially due to higher stress concentration on the column
411 under 100 kPa applied normal stress, which is the highest normal stress applied in this study.

412

Discussion

Typically, clays are highly sensitive to variation in their water content Spoor and Godwin (1979), and are marked by lower shear strength (Aslani et al., 2019). This study observed that the kaolin has the lowest direct shear strength. It was also noted that the inclusion of granular column increased the shear strength of the geocomposite, regardless of the type of column backfill, due to the combined soil-granular column system, which has been observed by several researchers before (Mohapatra et al., 2016). For example, reinforcing the kaolin with the CWG column under the applied normal stresses of 12.5, 25, 50 and 100 kPa increased the shear strength from 5.7, 9.9, 15.7 and 33.2 kPa to 8.9, 13.1, 29.9 and 49.3 kPa, respectively. As granular columns are formed by materials possessing relatively higher friction angle, the treated soil-column matrix manifest a higher friction angle than untreated soil, which is observed in the results presented in this study. Besides reinforcement, the increase in shear strength due to granular column inclusion could partly be due to the drainage ability of columns, causing a reduction in pore water pressure and an increase in effective stress of the soil (Najjar et al., 2010).

The obtained shear strength results reflect the overall response of the entire test specimens. The results showed that the increase in shear strength caused by the NS or the MS column is comparable to each other, showing close peak friction angle values of 17.8^{o} and 17.7^{o} for the NS-kaolin and the MS-kaolin geocomposite, respectively. The peak shear strength of the MS-kaolin geocomposite was higher than that of the NS-kaolin geocomposite. The potential reason for this finding could be the more well-graded gradation of MS, favouring the development of higher peak shear stress (Siahaan et al., 2018). Another potential reason could be the relatively higher angularity of the MS particles Kazmi et al. (2021), leading to a superior interlock between the MS particles. Naeini and Gholampoor (2019) investigated the shear strength behaviour of stone column-treated wet clays by installing ordinary stone columns and geotextile-encased stone columns using three different sizes of stones, ranging 1-2 mm, 2-5 mm and 5-8 mm. Their study found that the wet clay reinforced with columns containing coarser stones showed relatively greater shear strength than those containing smaller

aggregates, potentially due to the higher friction angle of coarser stones. Similarly, Bareither et al. (2008) analysed the physical properties and shear strength of 30 compacted sands sourced from a wide range of geological deposits. Their study concluded that sands with the highest friction angle tend to have coarser particles, well-graded gradation and/or angular particle shape. Hence, previous studies support the results of this paper, as MS-kaolin geocomposite showed a higher shear strength than that of the NS-kaolin geocomposite.

Installing the CWG column caused a relatively higher increase in the peak shear strength of the geocomposite under higher normal stresses; this is reflected in the results of the CWG-kaolin geocomposite, showing the highest friction angle and the lowest cohesion among the three geocomposites. For example, the shear strength mobilised by the CWG-kaolin geocomposite under 50 and 100 kPa normal stress were higher than that of the other two geocomposites. Secondly, installing the CWG column increased the friction angle from 14.0^{o} to 20.7^{o} (48% increase) compared to that of kaolin only specimens. This notable increase in the friction angle caused by installing the CWG column suggests that the frictional resistance offered by the CWG column was an important factor contributing to the overall increase in the shear strength of the CWG-kaolin geocomposite. Technically, there is a significant difference in the Young's modulus of glass compared to that of traditional sands. Literature shows that the Young's modulus of CWG particles is approximately 40 to 90 GPa (Hsieh et al., 2009; University of Texas, 2019; Qi et al., 2012; Karabulut et al., 2001; Engineering ToolBox, 2003), whereas that of sand and gravel particles typically varies from 10 to 170 MPa (University of Texas, 2019; Yamashita et al., 2000). The high shear strength of the CWG-kaolin geocomposite could be due to the higher stiffness (Young's modulus) of CWG particles compared with that of sands and gravels, leading to more stress being taken by the CWG column than the surrounding kaolin.

The post-shearing cross-section of the geocomposites under 25 kPa applied normal stress are given in Figure 11. These cross-sectional photos were taken by splitting the geocomposites along their vertical

axes to reveal the column and the surrounding kaolin. Upon careful examination of the geocomposites after shearing, it was noted that all three geocomposites underwent shear failure by lateral separation at the shearing plane. This finding complies with the previous literature, suggesting that a short column resting on a firm stratum typically fails in shear (Barksdale and Bachus, 1983). Further, it was observed that the CWG-kaolin geocomposite showed some signs of column bulging, largely at the centre. This finding supports the hypothesis that the CWG column attracted relatively higher stress concentration due to the mentioned higher stiffness of CWG particles, causing the CWG column to mobilise greater passive resistance from surrounding kaolin than the NS or MS column.

The use of encasement with granular columns is a fairly common technique to improve their performance, particularly in soft soils. Typically, geosynthetic materials (geotextiles and geogrids) are suited for use as encasements due to their superior tensile characteristics. Geosynthetic encasement could also improve the lateral load capacity of the granular column by developing hoop tension forces in the encasement layer, giving additional confinement to the column material (Mohapatra et al., 2016). As a result, they minimise the chances for bulging failure and for penetration of column material into the surrounding soil that could inhibit the drainage ability of the column (Dutta et al., 2016). As this study is among the first to investigate the performance of a granular column based on its type of column backfilling material (NS, MS or CWG), it was logical not to encase the granular column during the tests, providing benchmark results excluding the effect of the encasement. Previous studies also show that ordinary granular columns are prone to shear rupture under lateral soil movement and ideally need some encasement to reduce the chances of rupturing under shear loading (Murugesan and Rajagopal, 2009). Hence, future studies could consider investigating the direct shear behaviour of similar geocomposites with an encased column, particularly for granular columns made up of CWG. Moreover, it could also be helpful to perform some advanced characterisation testing on different sand, stone and CWG samples individually to help predict their behaviour as column backfill more accurately (Peng et al. 2020; Rueda et al. 2015; Serati et al. 2018). The next stage of this research will

present results showing the effect of particle size of CWG on the geotechnical behaviour of kaolin reinforced with a CWG column.

Conclusion

This study investigated the shear strength behaviour of column-kaolin geocomposites containing a column made up of NS, MS or CWG installed in the middle of the kaolin bed. Overall, installing a granular column increased the shear strength of the geocomposite, regardless of the type of column backfill used. It was observed that the increase in shear strength along the horizontal plane at the mid-height of the geocomposite inside the shear box caused by installing the NS or MS column was relatively comparable to each other, with the MS-kaolin geocomposite showing shear strength higher than that of the NS-kaolin geocomposite under all the applied normal stresses. A potential reason for this finding could be the well-graded gradation, higher particle angularity and larger median particle size of the MS than the NS. The results also showed that the CWG column is relatively more effective at increasing the peak shear strength of the geocomposite under higher normal stresses. It was noted that installing the CWG column led to the highest increase in the friction angle of the geocomposite. This could potentially be due to the higher stiffness of the CWG particles than that of NS or MS particles, causing greater stress concentration on the CWG column, ultimately leading to more stress being taken by the CWG column than the surrounding kaolin. Given the favourable performance demonstrated by the CWG column in this study, it is recommended to compare the experimental results of this study with field performance and large-scale physical model tests containing NS, MS or CWG columns. Secondly, this study suggests investigating the geotechnical behaviour of kaolin reinforced with groups of CWG columns. Given that this study is among the first to study the shear strength behaviour of CWG columns in clayey soil, it is also suggested for future researchers to study how CWG columns behave when encased with a suitable geosynthetic material. This study supports performing a detailed quantitative economic and environmental feasibility investigation for using CWG as column backfill in granular columns for future studies.

Data Availability Statement

All data, models, or code that support the findings of this study are available from the corresponding author upon reasonable request.

Acknowledgment

The authors would like to thank The University of Queensland (Australia) for providing the necessary resources to perform this research. We are also thankful to Mr Peter Lovegrove (Enviro Sand, Australia) for supplying crushed waste glass for this study. Special thanks go to Professor Alexander Scheuermann (School of Civil Engineering at The University of Queensland), Dr Zhongwei Chen (School of Mechanical and Mining Engineering at The University of Queensland) and Dr Denys Villa Gomez (School of Civil Engineering at The University of Queensland) for providing their constructive suggestions.

Notation

The following symbols are used in this paper:

LDS	Large direct shear test
NS	Natural sand
MS	Manufactured sand
CWG	Crushed waste glass
LDSM	Large direct shear test machine
LVDT	Linear variable differential transducers
S_U	Undrained shear strength
C_r	Column penetration ratio
PVC	Polyvinyl Chloride
A_r	Area replacement ratio
L/D ratio	Length to Diameter ratio
NSE	Nash-Sutcliffe model efficiency coefficient

Supplemental Materials

The UQ Researchers in this Video Abstract present the key motivations, analyses performed, and findings of a cross-institutional study comparing the behaviour of a weak soil reinforced with granular columns containing three different types of backfill materials. The study conducted shear strength testing using the advanced high-accuracy large direct shear machine available at The University of Queensland, Australia.

Performed in collaboration with University College London and Imperial College London in the UK, this study presents the shear strength performance of a weak soil reinforced with a crushed waste glass column and compared it with that containing a natural or quarried (manufactured) sand column. The article reveals new insights into the unexplored shear strength performance of crushed waste glass as backfill in a granular column. Another standalone contribution of this study is that it provides an insight into how the origin of sand could impact its shear strength behaviour in a granular column, as natural and manufactured sands are largely sourced from beaches or rivers and quarries, respectively.

In conclusion, the study found that crushed waste glass showed promising behaviour as an alternative geomaterial and could potentially be used to backfill granular columns, helping to offer a circular economy solution by reducing pressure on landfills, recycling growing waste glass stockpiles, and conserving depleting natural and quarried sand resources.

YouTube link to the video abstract: https://www.youtube.com/watch?v=PtaPirmPMdU

References

Abhishek, S., Rajyalakshmi, K., and Madhav, M. 2016. "Engineering of ground with granular piles: a critical review." International Journal of Geotechnical Engineering. 10(4): 337-357. https://doi.org/10.1080/19386362.2016.1145942.

Alfaro, M., Balasubramaniam, A., Bergado, D., and Chai, J. 1994. "Improvement techniques of soft ground in subsiding and lowland environment". CRC Press.

565 Ali, M. Y. 2012. "Geotechnical characteristics of recycled glass in road pavement applications."
566 Doctor of Philosophy (thesis), Swinburne University of Technology, Melbourne, Australia,
567 Alnunu, M. Z., and Nalbantoglu, Z. 2019. "Performance of loose sand with different waste materials
568 in stone columns in North Cyprus." Environmental Geotechnics.
569 https://doi.org/10.1680/jenge.18.00079.
570 Amini, R. 2016. "Physical modelling of vibro stone column using recycled aggregates." University of
571 Birmingham,
572 Andreou, P., Frikha, W., Frank, R., Canou, J., Papadopoulos, V., and Dupla, J. C. 2008. "Experimental
573 study on sand and gravel columns in clay." Proceedings of the Institution of Civil Engineers-
574 Ground Improvement. 161(4): 189-198. https://doi.org/10.1680/grim.2008.161.4.189.
575 Aslani, M., Nazariafshar, J., and Ganjian, N. 2019. "Experimental study on shear strength of cohesive
576 soils reinforced with stone columns." Geotechnical and Geological Engineering. 37(3): 2165-
577 2188. https://doi.org/10.1007/s10706-018-0752-z.
578 Ayothiraman, R., and Soumya, S. 2015. "Model tests on the use of tyre chips as aggregate in stone
579 columns." Proceedings of the Institution of Civil Engineers-Ground Improvement. 168(3):
580 187-193. https://doi.org/10.1680/grim.13.00006.
581 Babu, M. D., Nayak, S., and Shivashankar, R. 2013. "A critical review of construction, analysis and
582 behaviour of stone columns." Geotechnical and Geological Engineering. 31(1): 1-22.
583 https://doi.org/10.1007/s10706-012-9555-9.
584 Bareither, C. A., Edil, T. B., Benson, C. H., and Mickelson, D. M. 2008. "Geological and physical factors
585 affecting the friction angle of compacted sands." Journal of Geotechnical and
586 Geoenvironmental Engineering. 134(10): 1476-1489. https://doi.org/10.1061/(asce)1090-
587 0241(2008)134:10(1476).
588 Barksdale, R. D., and Bachus, R. C. 1983. "Design and construction of stone columns, volume I.

589 Barmade, S., Kale, V., and Gadekar, M. R. 2021. "Experimental Study on Load-Settlement Behaviour
590 of Granular Stone Column in Expansive Soil." Paper presented at the Proceedings of the
591 Indian Geotechnical Conference 2019. https://doi.org/10.1007/978-981-33-6444-8_76.
592 Bendixen, M., Best, J., Hackney, C., and Iversen, L. L. 2019. "Time is running out for sand." Nature
593 Publishing Group. https://doi.org/10.1038/d41586-019-02042-4.
594 Bergado, D., Singh, N., Sim, S., Panichayatum, B., Sampaco, C., and Balasubramaniam, A. 1990.
595 "Improvement of soft Bangkok clay using vertical geotextile band drains compared with
596 granular piles." Geotextiles and Geomembranes. 9(3): 203-231.
597 https://doi.org/10.1016/0266-1144(90)90054-g.
598 Bravo, M., De Brito, J., Pontes, J., and Evangelista, L. 2015. "Mechanical performance of concrete
599 made with aggregates from construction and demolition waste recycling plants." Journal of
600 Cleaner Production. 99: 59-74. https://doi.org/10.1016/j.jclepro.2015.03.012.
601 Canakci, H., Celik, F., and Edil, T. B. 2019. "Effect of sand column on compressibility and shear
602 strength properties of peat". European Journal of Environmental and Civil Engineering.
603 23(9): 1094-1105. https://doi.org/10.1080/19648189.2017.1344142.
604 Castro, J. 2017. "Modeling stone columns." Materials. 10(7). https://doi.org/10.3390/ma10070782.
605 Chawla, G., Raju, V., and Krishna, Y. 2010. "Some environmental benefits of dry vibro stone columns
606 in a gas based power plant project." Paper presented at the Indian Geotechnical Conference.
607 Mumbai, India.
608 Chiew, F., and McMahon, T. 1993. "Assessing the adequacy of catchment streamflow yield
609 estimates." Soil Research. 31(5): 665-680. https://doi.org/10.1071/sr9930665.
610 Clean Washington Center. 1996. "Best Practices in Glass Recycling - Analysis of Glass Dusts."
611 Retrieved from:
612 http://citeseerx.ist.psu.edu/viewdoc/download;jsessionid=8EA266C3CB54A9A2141B63AAB2EDBA2C
613 ?doi=10.1.1.384.5175&rep=rep1&type=pdf

614 Dash, S. K., and Bora, M. C. 2013. "Influence of geosynthetic encasement on the performance of
615 stone columns floating in soft clay." Canadian Geotechnical Journal. 50(7): 754-765.
616 https://doi.org/10.1139/cgj-2012-0437.
617 Dutta, S., Nadaf, M., Lal Birali, R. R., and Mandal, J. 2016. "Encased stone columns for soft ground
618 improvement." Geo-Chicago 2016. 746-755. https://doi.org/10.1061/9780784480144.074.
619 Egan, D., and Slocombe, B. 2010. "Demonstrating environmental benefits of ground improvement."
620 Proceedings of the Institution of Civil Engineers-Ground Improvement. 163(1): 63-69.
621 https://doi.org/10.1680/grim.2010.163.1.63.
622 Engineering ToolBox, (2003). Young's Modulus - Tensile and Yield Strength for some common
623 Materials. [online] Available at: https://www.engineeringtoolbox.com/young-modulus-
624 d_417.html (Accessed on 7 Oct 2021).
625 Gourley, C., Newill, D., and Schreiner, H. 2020. "Expansive soils: TRL's research strategy." Engineering
626 Characteristics of Arid Soils. 247-260. CRC Press. https://doi.org/10.1201/9781003077787-
627 28.
628 Hanna, A., Etezad, M., and Ayadat, T. 2013. "Mode of failure of a group of stone columns in soft
629 soil." International Journal of Geomechanics. 13(1): 87-96.
630 https://doi.org/10.1061/(asce)gm.1943-5622.0000175.
631 Holmstrom, O. C., and Swan, C. W. 1999. "Geotechnical properties of innovative, synthetic
632 lightweight aggregates." Paper presented at the Proceedings of the 1999 International Ash
633 Utilization Symposium.
634 Hsieh, P., Lin, S., Su, H., and Jang, J. 2009. "Glass forming ability and mechanical properties
635 characterization on Mg58Cu31Y11− xGdx bulk metallic glasses." Journal of alloys and
636 compounds 483(1-2): 40-43. https://doi.org/10.1016/j.jallcom.2008.08.124.
637 Karabulut, Melnik, Stefan, Marasinghe, Ray, Kurkjian, and Day. (2001). Mechanical and structural
638 properties of phosphate glasses. *Journal of Non-Crystalline Solids, 288*(1-3), 8-17.

639 Kazmi, Serati, Williams, Qasim, and Cheng. 2021. "The potential use of crushed waste glass as a
640 sustainable alternative to natural and manufactured sand in geotechnical applications." Journal of
641 Cleaner Production. 284, 124762. https://doi.org/10.1016/j.jclepro.2020.124762.
642 Kazmi, Serati, Williams, Qasim, Cheng, and Olaya. 2020. "A Comparative Study on Shear Strength of
643 Crushed Waste Glass with Natural and Manufactured Sand." Paper presented at the 54th US
644 Rock Mechanics/Geomechanics Symposium.
645 Kazmi, Williams, and Serati. 2019. "Comparison of Basic Geotechnical Parameters of Crushed Waste
646 Glass with Natural and Manufactured Sands." Paper presented at the 53rd US Rock
647 Mechanics/Geomechanics Symposium.
648 Kazmi, Williams, and Serati. 2020. "Waste glass in civil engineering applications—A
649 review." International Journal of Applied Ceramic Technology. 17(2): 529-554.
650 https://doi.org/10.1111/ijac.13434.
651 Kumar, A., and Sadana, D. 2012. "Bearing capacity of soil reinforced with vertical columns of recycled
652 concrete aggregates." Australian Journal of Civil Engineering 10(2): 153-162.
653 https://doi.org/10.7158/c11-704.2012.10.2
654 Langer, W., Drew, L., and Sachs, J. 2004. "Aggregate and the environment: American Geological
655 Institute Environmental Awareness". Series No. 8. American Geological Institute, Alexandria,
656 64.
657 Malarvizhi, S. 2007. "Comparative study on the behavior of encased stone column and conventional
658 stone column." Soils and foundations. 47(5): 873-885. https://doi.org/10.3208/sandf.47.873.
659 Manohar, R., and Patel, S. 2021. "Ground Improvement with Stone Columns–A Review." Advances in
660 Civil Engineering. 197-217. Springer. https://doi.org/10.1007/978-981-15-5644-9_14.
661 McCabe, B. A., McNeill, J. A., and Black, J. A. 2007. "Ground improvement using the vibro-stone
662 column technique." The Institution of Engineers of Ireland.

663 Mehrannia, N., Kalantary, F., and Ganjian, N. 2018. "Experimental study on soil improvement with
664 stone columns and granular blankets." Journal of Central South University. 25(4): 866-878.
665 https://doi.org/10.1007/s11771-018-3790-z.
666 Mishra, Bore, Jiang, Scheuermann, and Li. 2018a. "Dielectric spectroscopy measurements on kaolin
667 suspensions for sediment concentration monitoring." Measurement. 121: 160-169.
668 https://doi.org/10.1016/j.measurement.2018.02.034.
669 Mishra, Scheuermann, and Li. 2018b. "Significance of corrections and impact of saline pore fluid on
670 kaolin." Journal of Materials in Civil Engineering. 30(11), 06018016.
671 https://doi.org/10.1061/(asce)mt.1943-5533.0002458.
672 Mishra, Zhang, Bhuyan, and Scheuermann. 2020. "Anisotropy in volume change behaviour of soils
673 during shrinkage." Acta Geotechnica. 15(12): 3399-3414. https://doi.org/10.1007/s11440-
674 020-01015-6.
675 Mohapatra, S. R., Rajagopal, K., and Sharma, J. 2014. "Analysis of geotextile-reinforced stone
676 columns subjected to lateral loading." Paper presented at the Proc. 10th Int. Conf. on
677 Geosynthetics, Berlin, Germany.
678 Mohapatra, S. R., Rajagopal, K., and Sharma, J. 2016. "Direct shear tests on geosynthetic-encased
679 granular columns." Geotextiles and Geomembranes. 44(3): 396-405.
680 https://doi.org/10.1016/j.geotexmem.2016.01.002.
681 Mokhtari, M., and Kalantari, B. 2012. "Soft Soil Stabilization using Stone Column--A Review."
682 Electronic journal of Geotechnical engineering. 17: 1459-1466.
683 Murugesan, S., and Rajagopal, K. 2007. "Model tests on geosynthetic-encased stone columns."
684 Geosynthetics International. 14(6): 346-354. https://doi.org/10.1680/gein.2007.14.6.346.
685 Murugesan, S., and Rajagopal, K. 2009. "Shear load tests on stone columns with and without
686 geosynthetic encasement." Geotechnical Testing Journal. 32(1): 76-85.
687 https://doi.org/10.1520/gtj101219.

688 Naeini, S. A., and Gholampoor, N. 2019. "Effect of Geotextile Encasement on the Shear Strength
689 Behavior of Stone Column-Treated Wet Clays." Indian Geotechnical Journal. 49(3): 292-303.
690 https://doi.org/10.1007/s40098-018-0329-z.
691 Najjar, S. S. 2013. "A state-of-the-art review of stone/sand-column reinforced clay systems."
692 Geotechnical and Geological Engineering. 31(2): 355-386. https://doi.org/10.1007/s10706-
693 012-9603-5.
694 Najjar, S. S., Sadek, S., and Maakaroun, T. 2010. "Effect of sand columns on the undrained load
695 response of soft clays." Journal of Geotechnical and Geoenvironmental Engineering. 136(9):
696 1263-1277. https://doi.org/10.1061/(asce)gt.1943-5606.0000328.
697 Ng, K., and Tan, S. 2015. "Stress transfer mechanism in 2D and 3D unit cell models for stone column
698 improved ground." International Journal of Geosynthetics and Ground Engineering. 1(1): 1-9.
699 https://doi.org/10.1007/s40891-014-0003-1.
700 Peng, Y., Ding, X., Xiao, Y., Deng, X., and Deng, W. 2020. "Detailed amount of particle breakage in
701 multi-sized coral sands under impact loading." European Journal of Environmental and Civil
702 Engineering. 1-10. https://doi.org/10.1080/19648189.2020.1762750.
703 Poorooshasb, H., and Meyerhof, G. 1997. "Analysis of behavior of stone columns and lime columns."
704 Computers and Geotechnics. 20(1): 47-70. https://doi.org/10.1016/s0266-352x(96)00013-4.
705 Priebe, H. J. 1995. "The design of vibro replacement". Ground engineering. 28(10): 1-9.
706 Qi, Tessier-Doyen, and Absi. (2012). Young's modulus evolution with temperature of glass/andalusite
707 model materials: Experimental and numerical approach. *Computational Materials Science,*
708 *55*, 44-53.
709 Ranjan, G. 1989. "Ground treated with granular piles and its response under load." Indian
710 Geotechnical Journal. 19(1): 1-86.
711 Rossato, G., Ninis, N. L., and Jardine, R. J. 1992. "Properties of some kaolin-based model clay soils."
712 Geotechnical Testing Journal. 15(2): 166-179. https://doi.org/10.1520/gtj10238j.

713 Rueda, J., Dapena, E., Alaejos, P., and de Llano, S. M. 2015. "An accelerated test to assess the quality
714 of recycled concrete sands based on their absorption capacity." Construction and Building
715 Materials. 78: 464-469. https://doi.org/10.1016/j.conbuildmat.2014.12.039.
716 Saberian, M., Li, J., and Cameron, D. 2019. "Effect of crushed glass on behavior of crushed recycled
717 pavement materials together with crumb rubber for making a clean green base and
718 subbase." Journal of Materials in Civil Engineering. 31(7), 04019108.
719 https://doi.org/10.1061/(asce)mt.1943-5533.0002765.
720 Serati, M., Masoumi, H., Williams, D., Alehossein, H., and Roshan, H. 2018. "Some new aspects on
721 the diametral point load testing." 52nd US Rock Mechanics/Geomechanics Symposium.
722 ARMA-2018-1025.
723 Serridge, C. 2004. "THE USE OF RECYCLED AGGREGATES IN VIBRO STONE COLUMN GROUND
724 IMPROVEMENT TECHNIQUES." Sustainable Waste Management and Recycling: Construction
725 Demolition Waste (pp. 213-224): Thomas Telford Publishing.
726 Serridge, C., and Sarsby, R. 2009. "Assessment of the use of recycled aggregates in vibro-stone
727 column ground improvement techniques." In Construction for a Sustainable Environment
728 (pp. 86-101): CRC Press. https://doi.org/10.1201/9780203856918-8.
729 Serridge, and Slocombe. 2012. "Chapter 84 Ground improvement ICE manual of geotechnical
730 engineering (pp. 1247-1269): Thomas Telford Ltd.
731 Schanz, and Vermeer. (1998). On the stiffness of sands *Pre-failure deformation behaviour of*
732 *geomaterials* (pp. 383-387): Thomas Telford Publishing.
733 Shahverdi, M., and Haddad, A. 2020. "Use of recycled materials in floating stone columns."
734 Proceedings of the Institution of Civil Engineers-Construction Materials. 173(2): 99-108.
735 https://doi.org/10.1680/jcoma.18.00086.
736 Siahaan, F., Indraratna, B., Ngo, N. T., Rujikiatkamjorn, C., and Heitor, A. 2018. "Influence of particle
737 gradation and shape on the performance of stone columns in soft clay." Geotechnical
738 Testing Journal. 41(6): 1076-1091. https://doi.org/10.1520/gtj20160234.

739 Sivakumar, V., O'Kelly, B., Moorhead, C., Madhav, M., and Mackinnon, P. 2014. "Effectiveness of
740 granular columns in containing settlement." Proceedings of the institution of civil engineers-
741 geotechnical engineering. 167(4): 371-379. https://doi.org/10.1680/geng.12.00133.
742 Spoor, G., and Godwin, R. 1979. "Soil deformation and shear strength characteristics of some clay
743 soils at different moisture contents." Journal of Soil Science. 30(3): 483-498.
744 https://doi.org/10.1111/j.1365-2389.1979.tb01003.x.
745 University of Texas. 2019. "Some Useful Numbers on the Engineering Properties of Materials
746 (Geologic and Otherwise) GEOL 615." Retrieved from: https://www.jsg.utexas.edu/tyzhu/files/Some-
747 Useful-Numbers.pdf
748 Wroth, C., and Wood, D. 1978. "The correlation of index properties with some basic engineering
749 properties of soils." Canadian Geotechnical Journal. 15(2): 137-145.
750 https://doi.org/10.1139/t78-014.
751 Xu, Y., Methiwala, J., Williams, D. J., and Serati, M. 2018. "Strength and consolidation characteristics
752 of clay with geotextile-encased sand column." Proceedings of the Institution of Civil
753 Engineers-Ground Improvement. 171(3): 125-134. https://doi.org/10.1680/jgrim.17.00070.
754 Yamashita, Jamiolkowski, and Presti. (2000). Stiffness nonlinearity of three sands. *Journal of*
755 *Geotechnical and Geoenvironmental Engineering, 126*(10), 929-938.
756 Zukri, A., and Nazir, R. 2018. "Sustainable materials used as stone column filler: A short review."
757 Paper presented at the IOP Conference Series: Materials Science and Engineering.
758 https://doi.org/10.1088/1757-899x/342/1/012001.

Tables

Table 1. Results of mineralogical analysis performed using XRF spectroscopy (Kazmi et al., 2021).

Oxide concentration	Units	Natural sand	Manufactured sand	Crushed waste glass
SiO_2	%	99.81	67.74	72.07
TiO_2	%	0.06	0.67	0.05
Al_2O_3	%	<0.01	16.17	1.45
Fe_2O_3	%	0.05	5.81	0.34
MnO	%	<0.01	0.12	0.01
MgO	%	0.03	2.13	0.69
CaO	%	0.01	1.38	11.09
Na_2O	%	<0.01	1.71	13.73
K_2O	%	0.01	3.72	0.33
P_2O_5	%	91.07	0.16	0.03
SO_3	%	82.43	0.24	0.09
V_2O_5	ppm	9	177	20
Cr_2O_3	ppm	11	97	539
ZnO	ppm	5	122	72
SrO	ppm	2	133	155
BaO	ppm	26	920	355
Co_3O_4	ppm	42	18	26
NiO	ppm	8	42	4
CuO	ppm	<2	37	4

762 **Table 2.** Geotechnical parameters of the materials (Adapted from Kazmi et al. (2021) and Xu et al.
763 (2018))

Parameter	NS	MS	CWG	Kaolin	Standards
C_u	1.43	13.37	2.21	-	-
C_c	0.94	1.51	0.96	-	-
Minimum dry density (dry placement method) (kg/m^3)	1540	1690	1390	-	AS 1289.5.5.1–1998
Maximum dry density (Wet placement method) (kg/m^3)	1650	1960	1820	-	AS 1289.5.5.1–1998
Hydraulic conductivity (m/s)	3.81×10^{-4}	3.59 x 10-4	4.01 x 10-4	-	ASTM D2434-68
Abrasion loss (%)	6.00	9.60	2.40	-	ASTM D7428
Critical-state friction angle under dry conditions (^{o})	31.1	44.1	29.1	-	AS 1289.6.2.2-1998
Critical-state friction angle under saturated conditions (^{o})	30.7	41.3	32.4	-	AS 1289.6.2.2-1998
Particle roundness index	0.55 (Rounded)	0.24 (Sub-angular)	0.32 (Sub-rounded)	-	-
Specific gravity	2.63	2.74	2.50	2.61	ASTM D5550
Median particle size (mm)	0.29	1.55	1.42	0.0012	AS 1289.3.6.1-2009
Liquid limit (%)	-	-	-	90	ASTM D4318 - 10
Plastic limit (%)	-	-	-	35	ASTM D4318 - 10
Plasticity index (%)	-	-	-	55	ASTM D4318 - 10
F_{200} (%)	-	-	-	69	
Unified soil classification system (USCS) rating	SP	SW	SP	CH	ASTM D2487 - 06

764

765 **Table 3.** Comparison of the shear strength of kaolin with geocomposites

	Kaolin only	NS-kaolin geocomposite	MS-kaolin geocomposite	CWG-kaolin geocomposite
Cohesion (kPa)	1.7	3.9	5.4	3.1
Angle of internal friction (^{o})	14.0	17.8	17.7	20.7

Figure captions

Fig.1. Installation of the granular column through dry bottom-feed technique (Adapted from Serridge and Slocombe (2012))

Fig.2. Optical microscopic images of NS, MS and CWG (from left to right)

Fig.3. Gradation curve of the test materials (Adapted from Kazmi et al. (2021) and Xu et al. (2018))

Fig.4. Large direct shear machine (Wille Geotechnik ADS-300)

Fig.5a. Typical plan of the geocomposite

Fig.5b. Typical cross-section of the geocomposite

Fig.6a. Experimental set up prepared in the shear box for the kaolin only specimen

Fig.6b. Experimental set up prepared in the shear box for the NS-kaolin geocomposite

Fig.6c. Experimental set up prepared in the shear box for the MS-kaolin geocomposite

Fig.6d. Experimental set up prepared in the shear box for the CWG-kaolin geocomposite

Fig.7. Peak shear strength envelopes of the kaolin only specimens and the geocomposites

Fig.8a. Shear stress-horizontal displacement behaviour of the kaolin only specimens

Fig.8b. Shear stress-horizontal displacement behaviour of the NS-kaolin geocomposites

Fig.8c. Shear stress-horizontal displacement behaviour of the MS-kaolin geocomposites

Fig.8d. Shear stress-horizontal displacement behaviour of the CWG-kaolin geocomposites

Fig.9a. Horizontal-vertical displacement behaviour of the kaolin only specimens

Fig.9b. Horizontal-vertical displacement behaviour of the NS-kaolin geocomposites

Fig.9c. Horizontal-vertical displacement behaviour of the MS-kaolin geocomposites

Fig.9d. Horizontal-vertical displacement behaviour of the CWG-kaolin geocomposites

Fig.10. Maximum vertical displacement-normal stress behaviour of the specimens

Fig.11. Post-shearing cross-section of the geocomposites under 25 kPa applied normal stress (the NS-kaolin, the MS-kaolin and CWG-kaolin geocomposites from left to right)

Figure 1

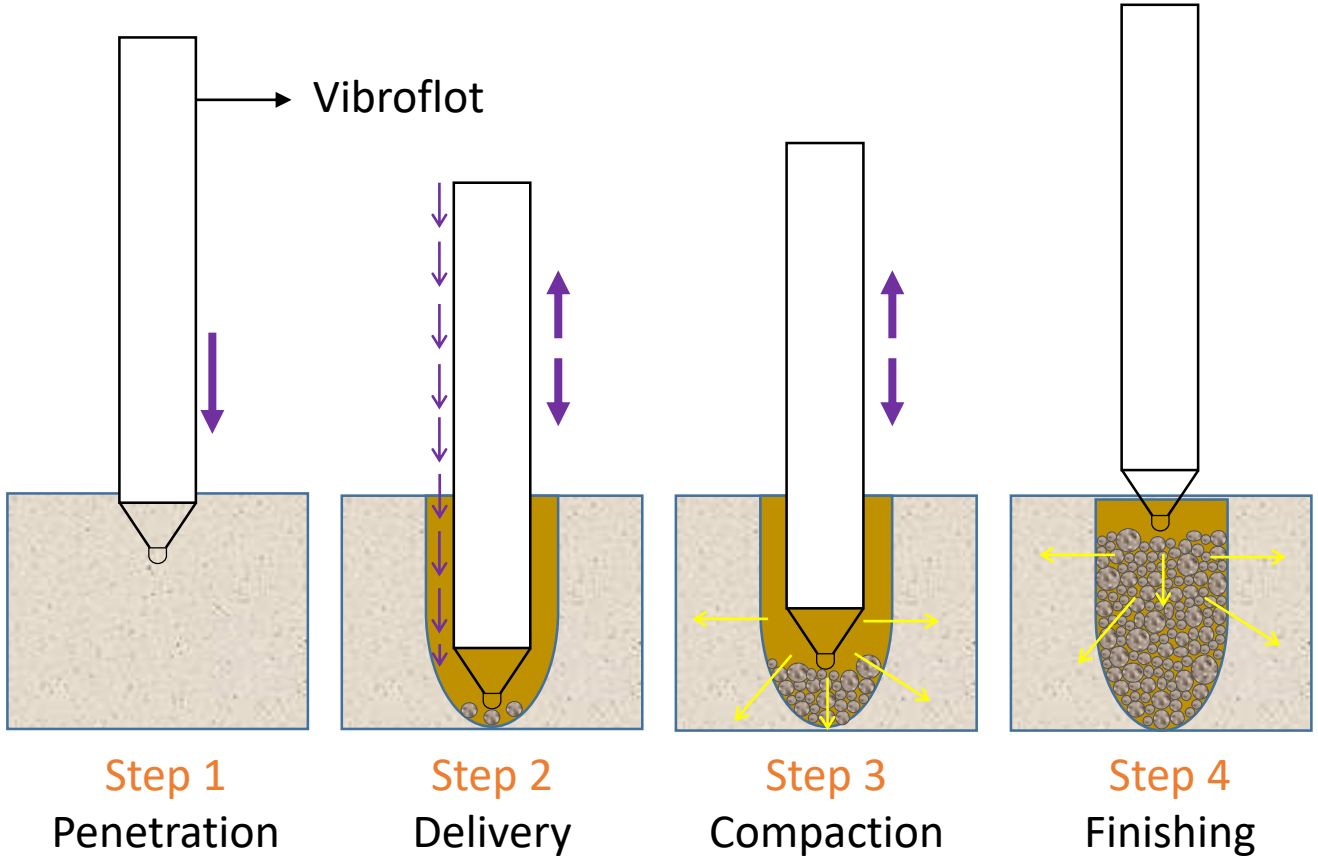

Figure 2

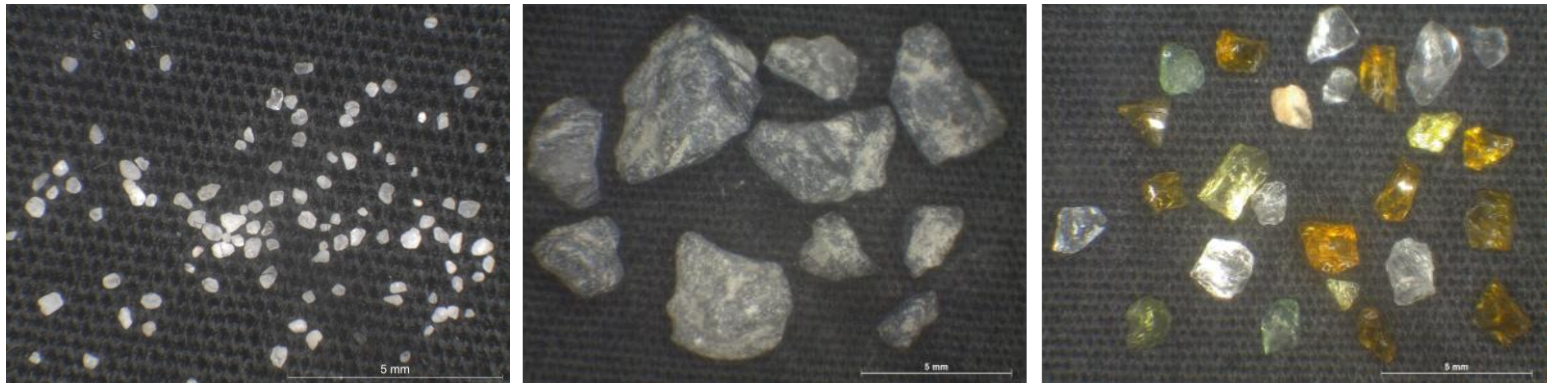

Figure 3

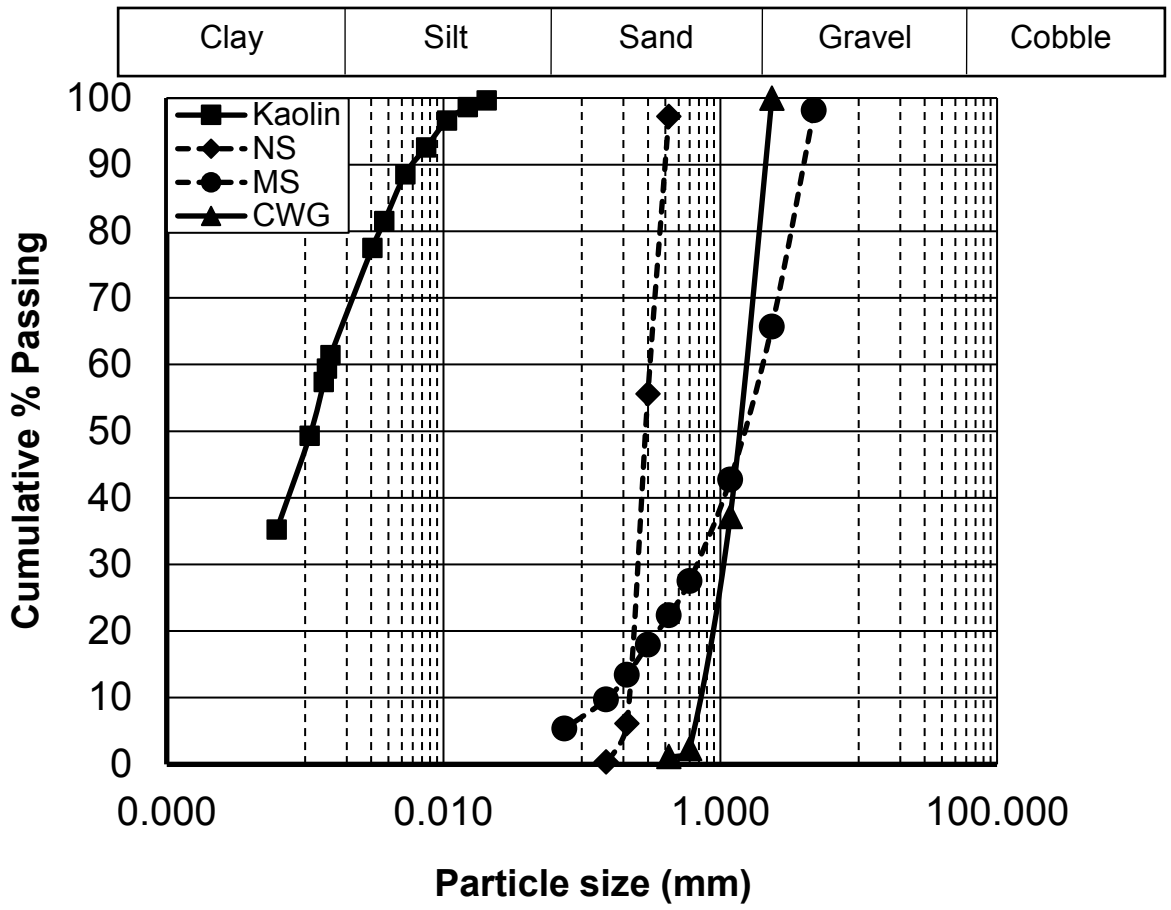

Figure 4

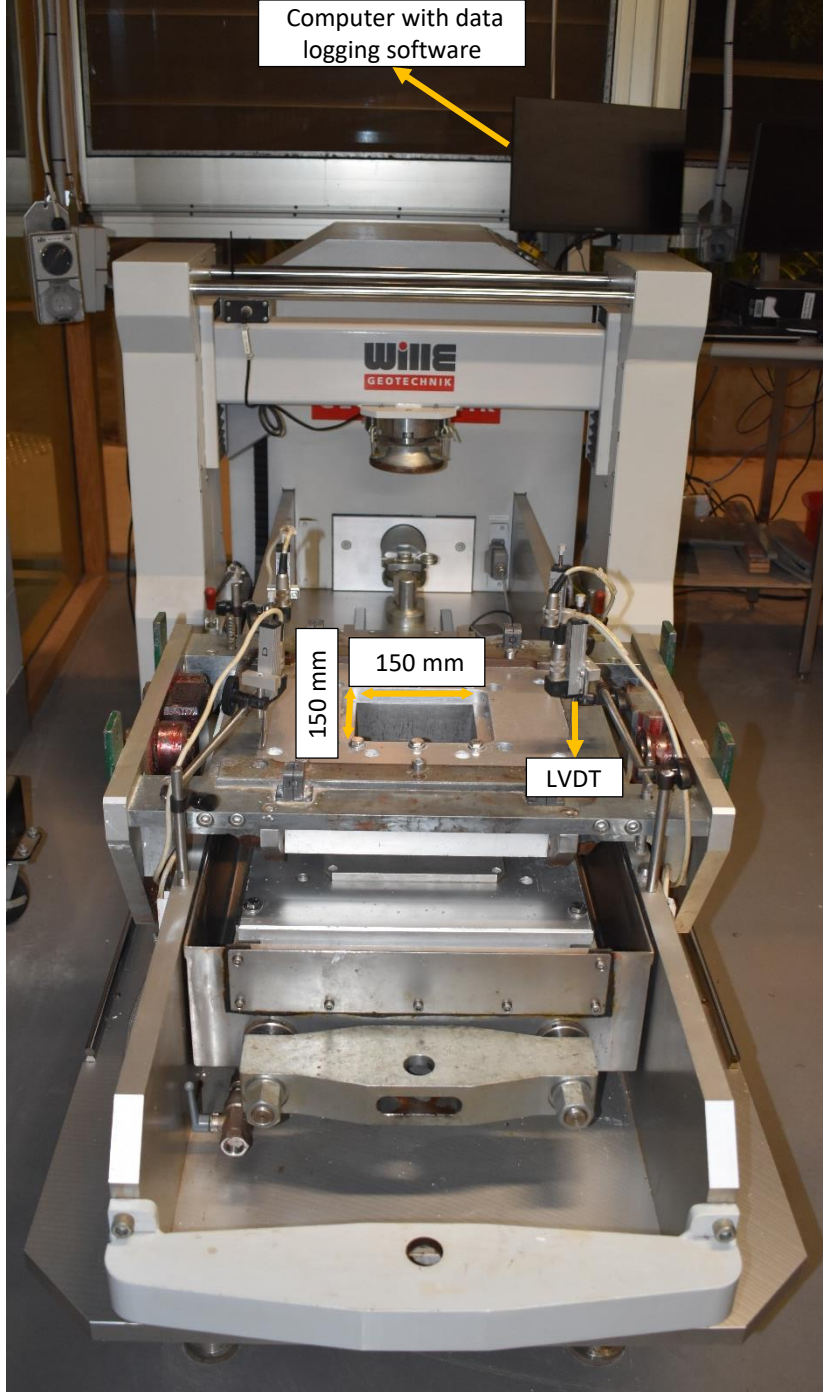

Figure 5a

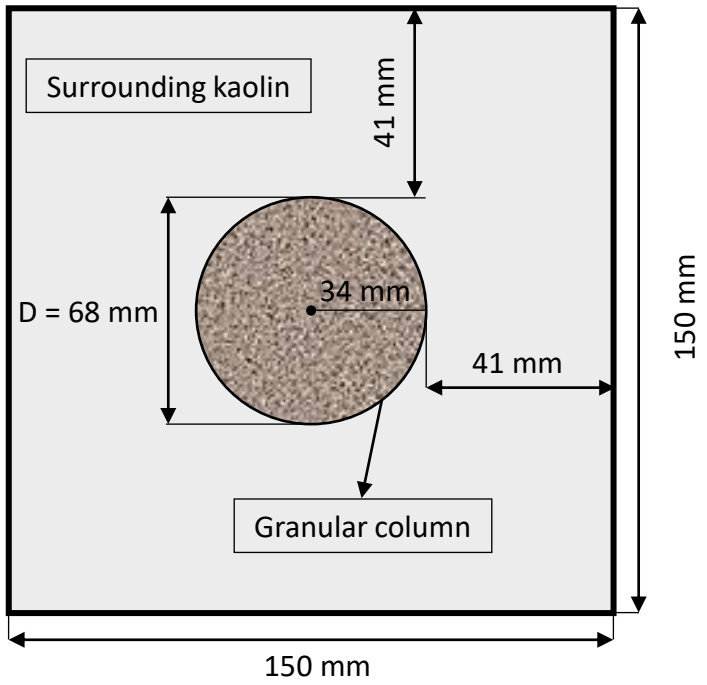

Figure 5b

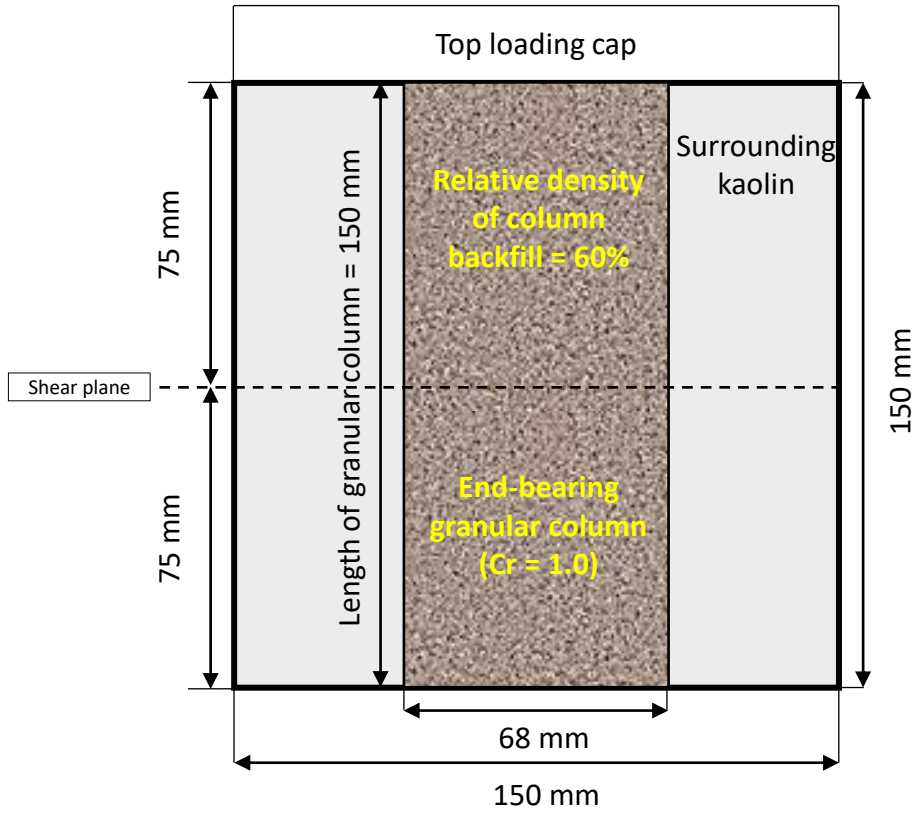

Figure 6a

Click here to access/download;Figure;Figure 6a.pdf

Figure 6b

Click here to access/download;Figure;Figure 6b.pdf

Figure 6c

Click here to access/download;Figure;Figure 6c.pdf

Figure 6d

Click here to access/download;Figure;Figure 6d.pdf

Figure 7

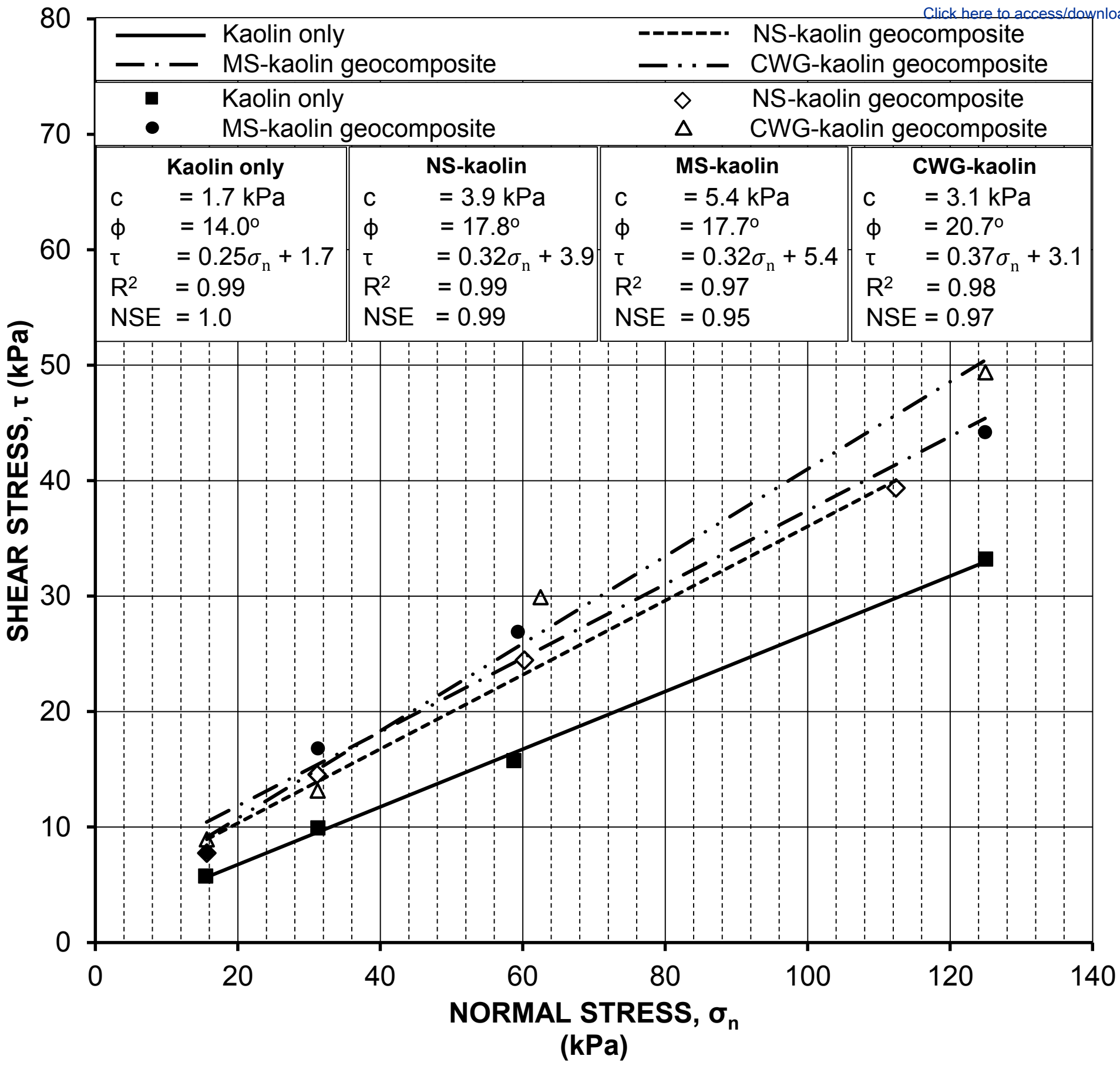

Figure 8a

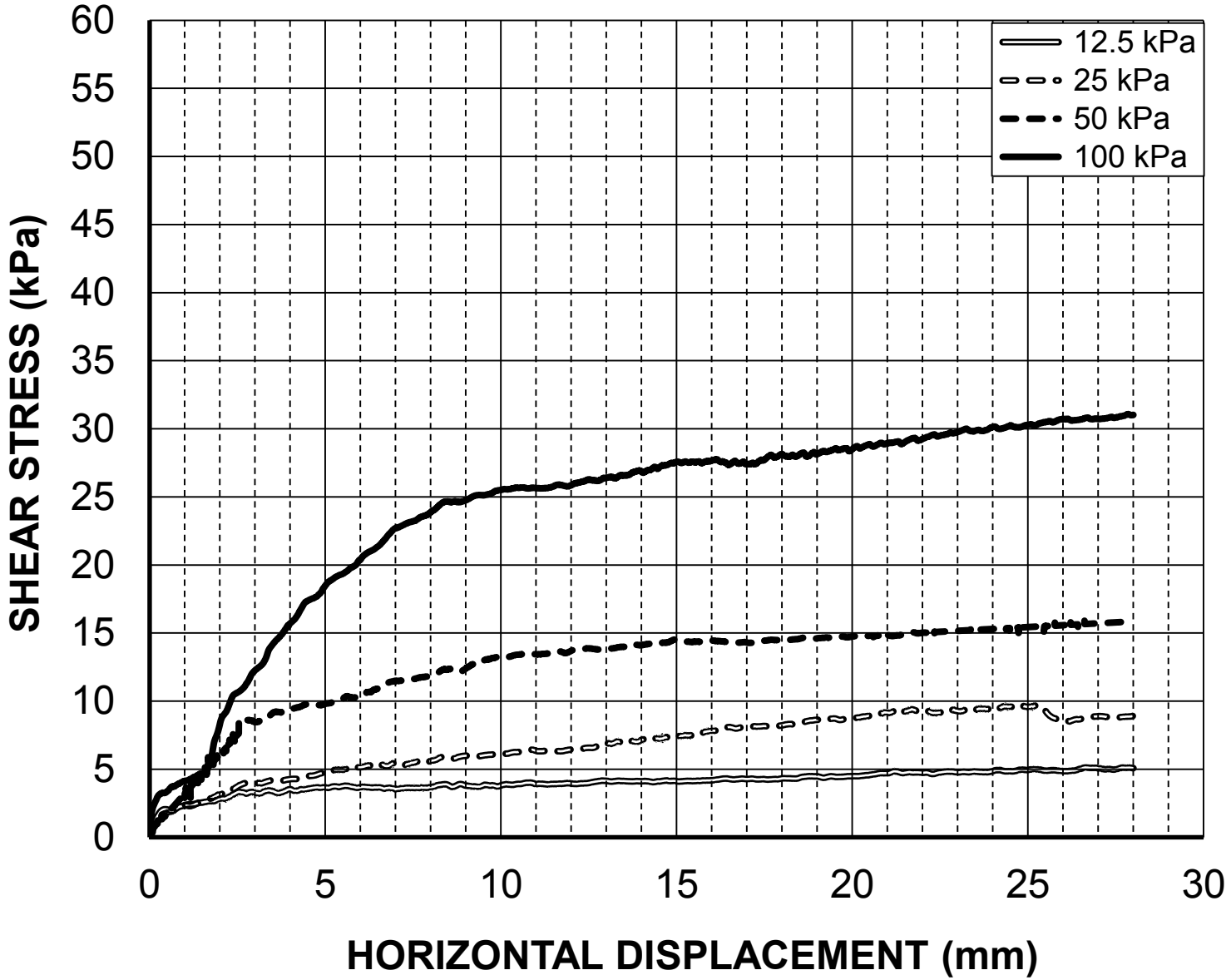

Figure 8b

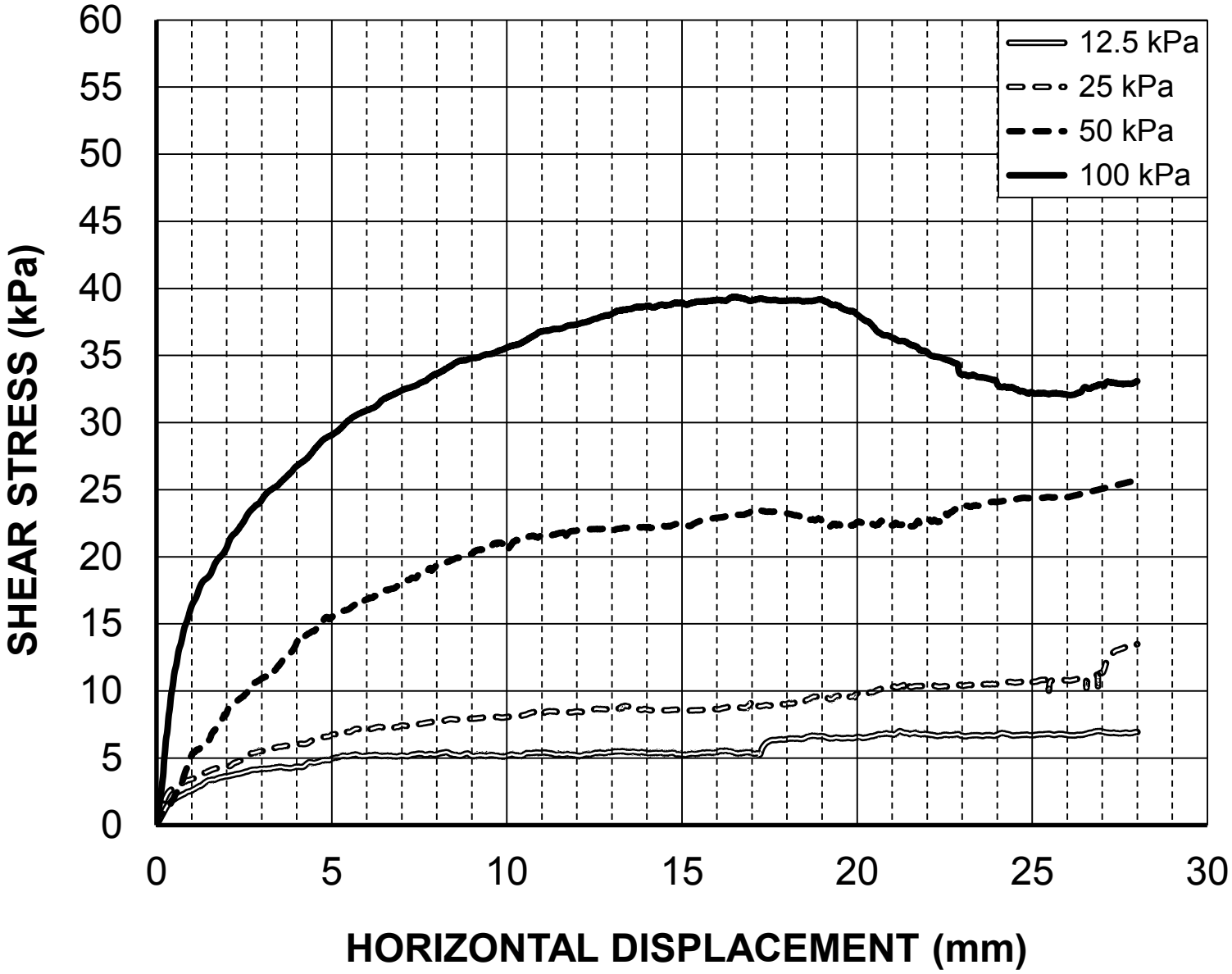

Figure 8c

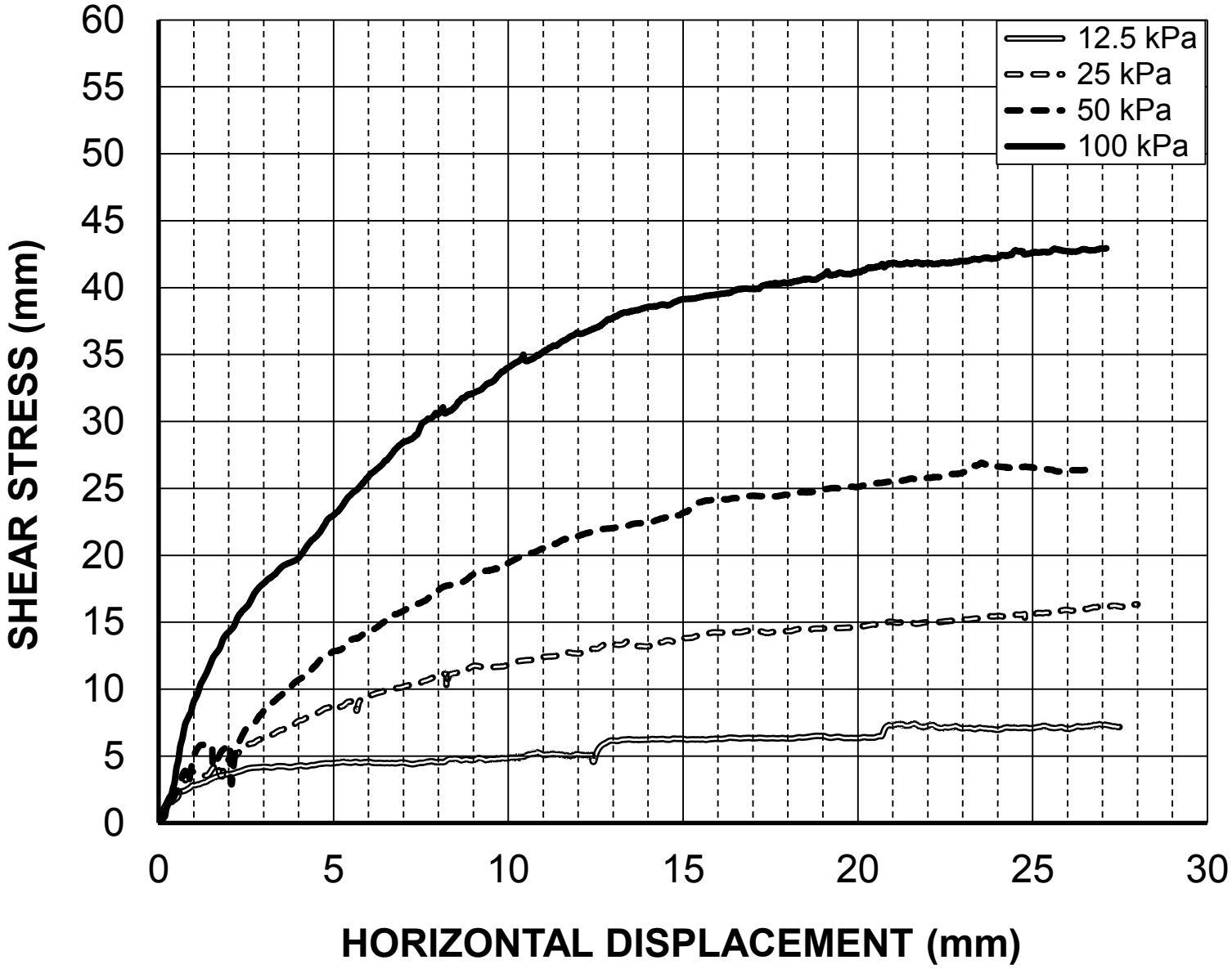

Figure 8d

Click here to access/download;Figure;Figure 8d.pdf

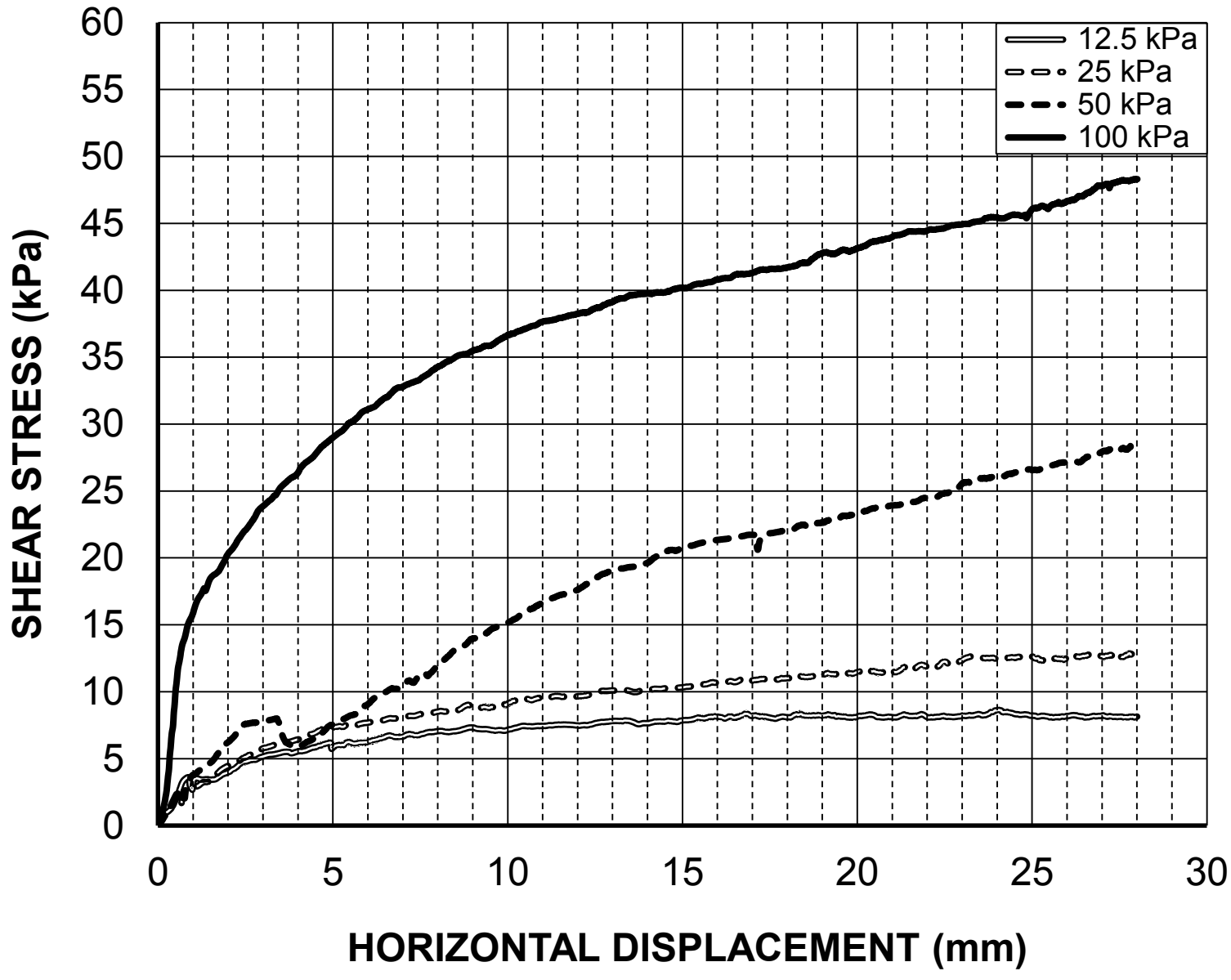

Figure 9a

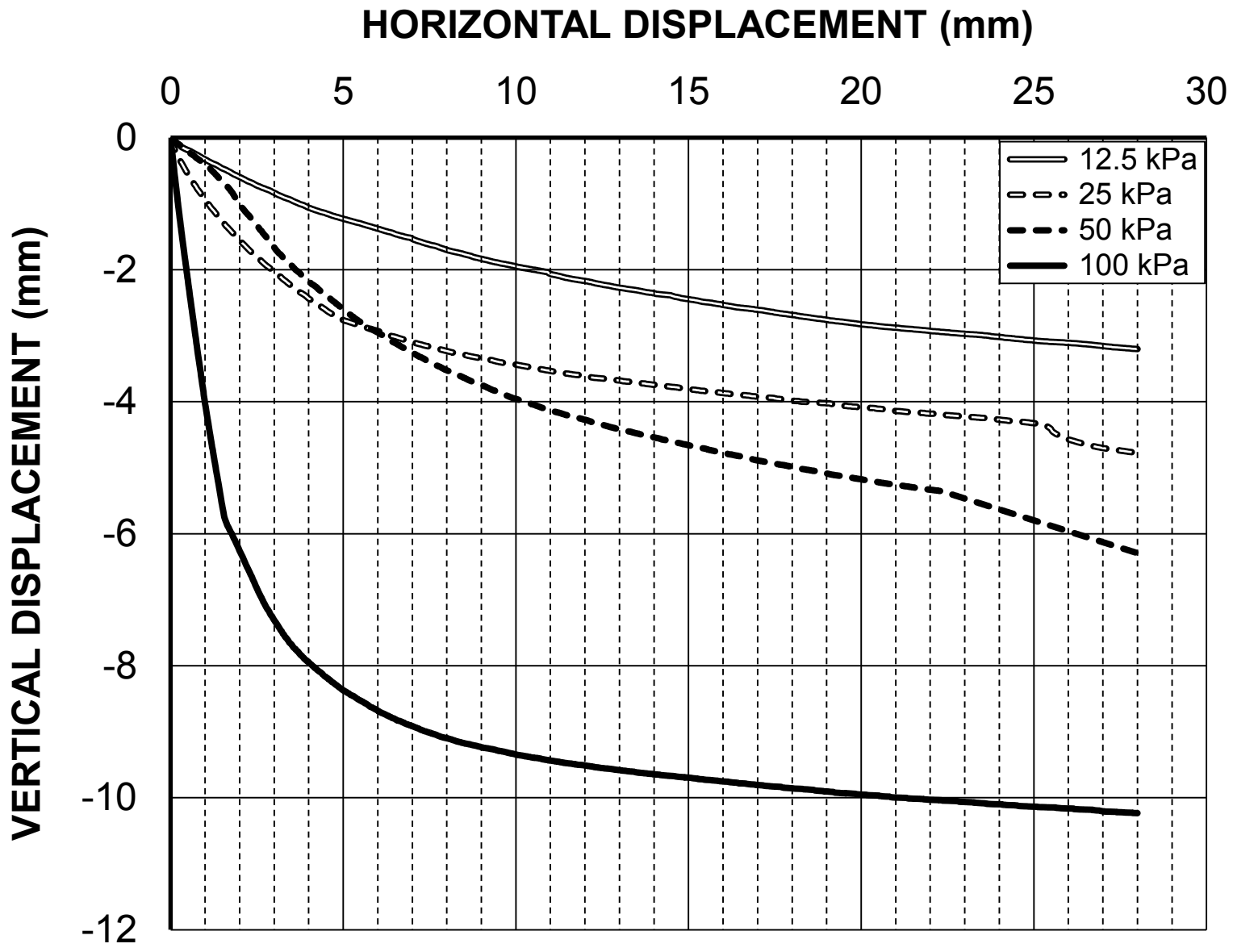

Figure 9b

Click here to access/download;Figure;Figure 9b.pdf

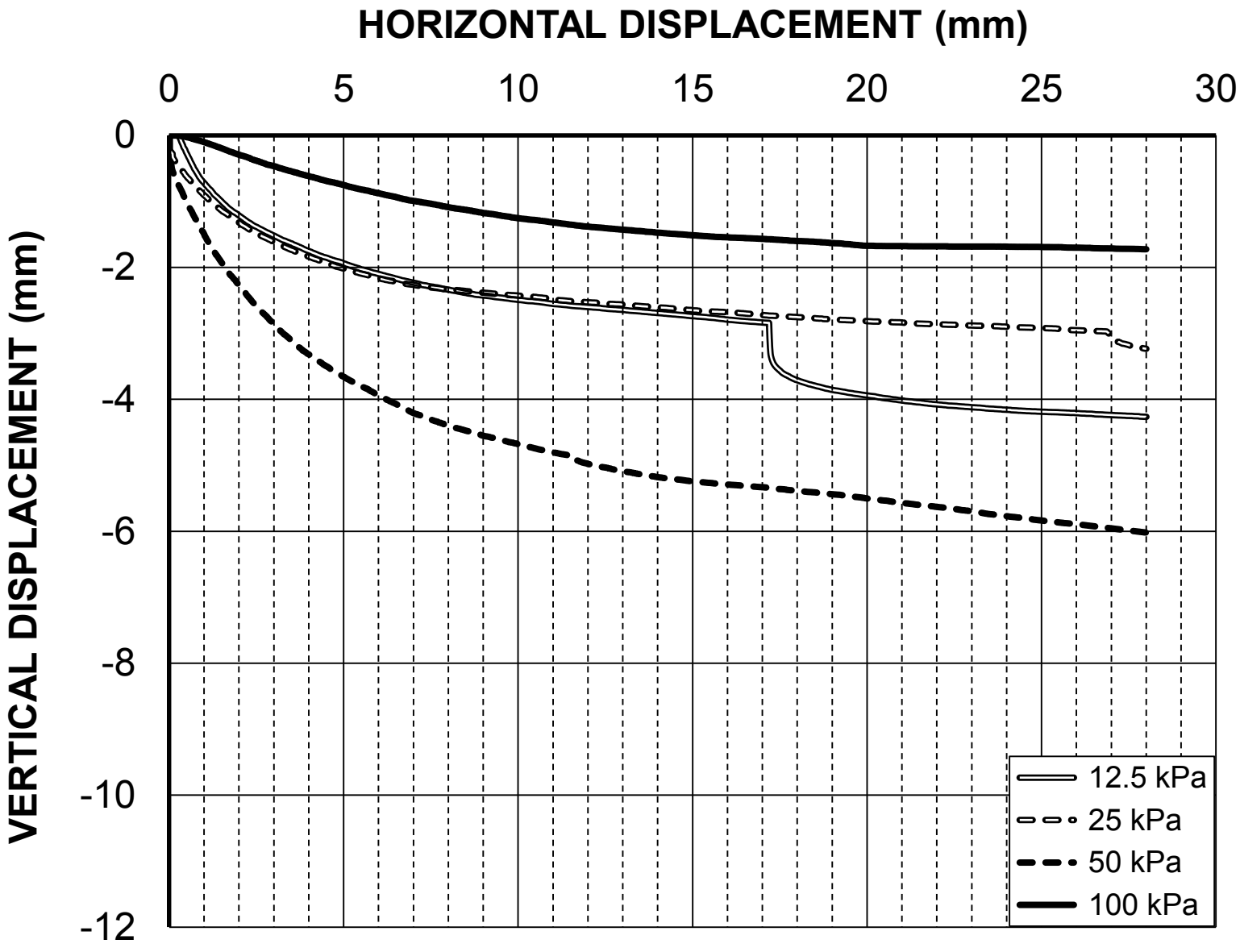

Figure 9c

Click here to access/download;Figure;Figure 9c.pdf

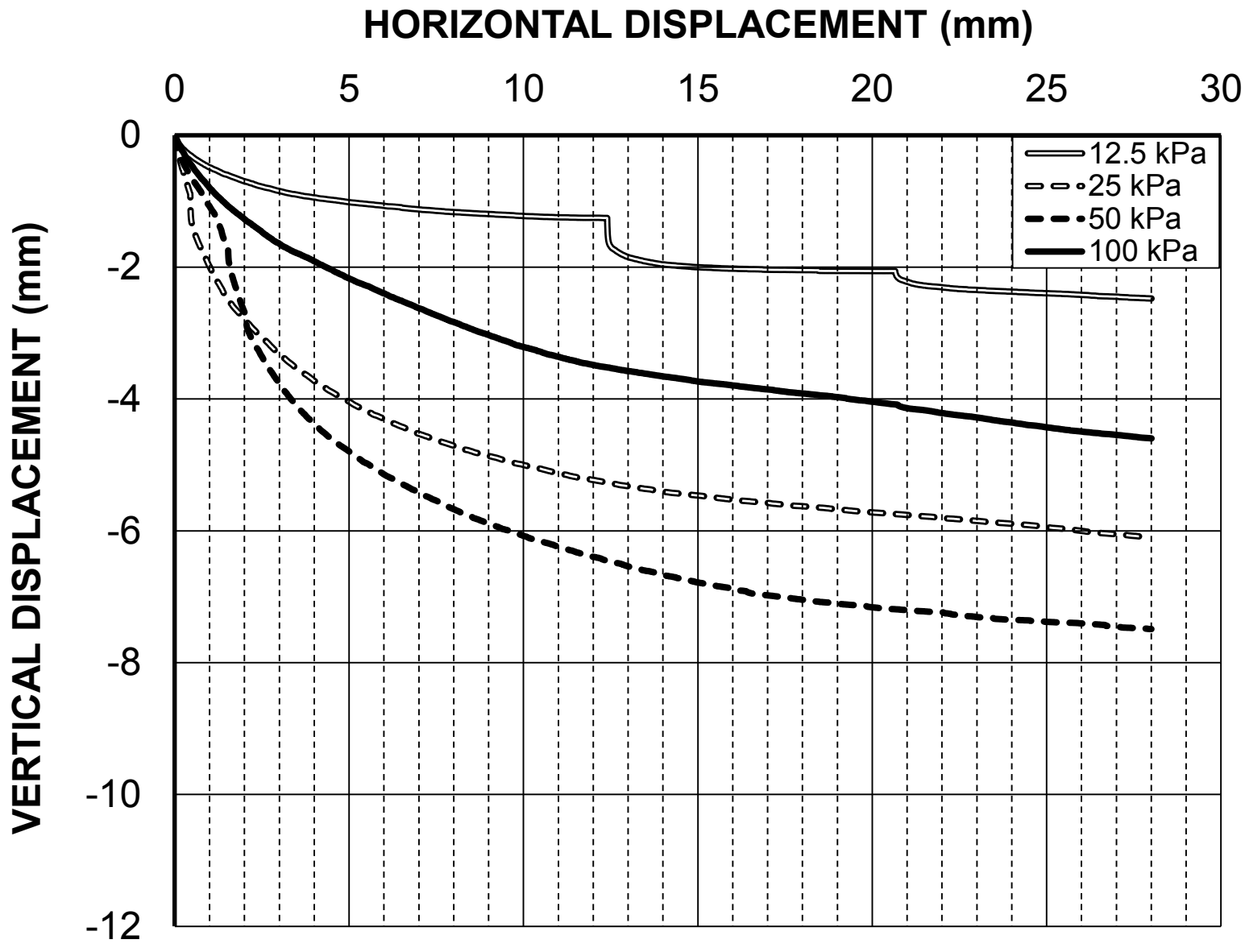

Figure 9d

Click here to access/download;Figure;Figure 9d.pdf

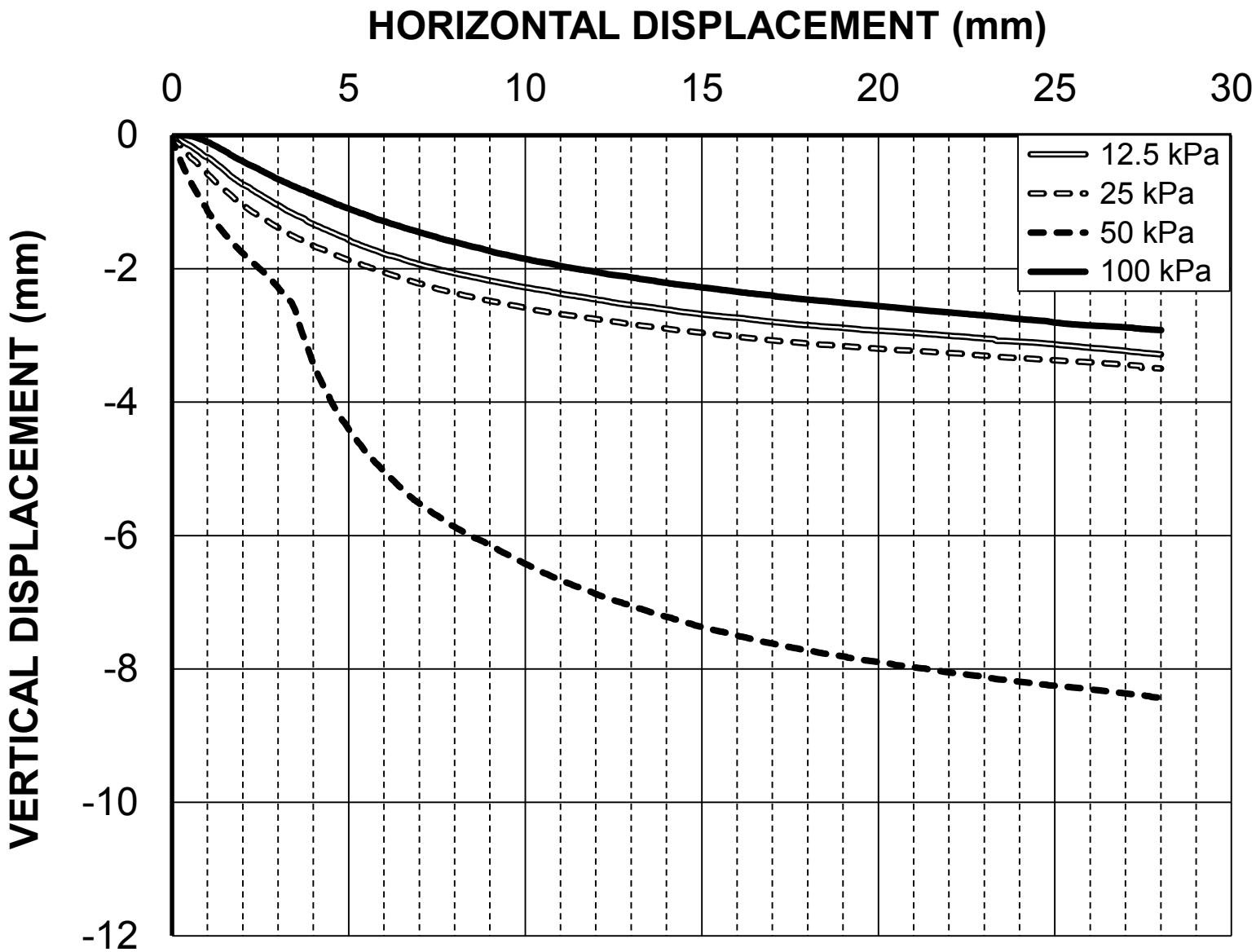

Figure 10

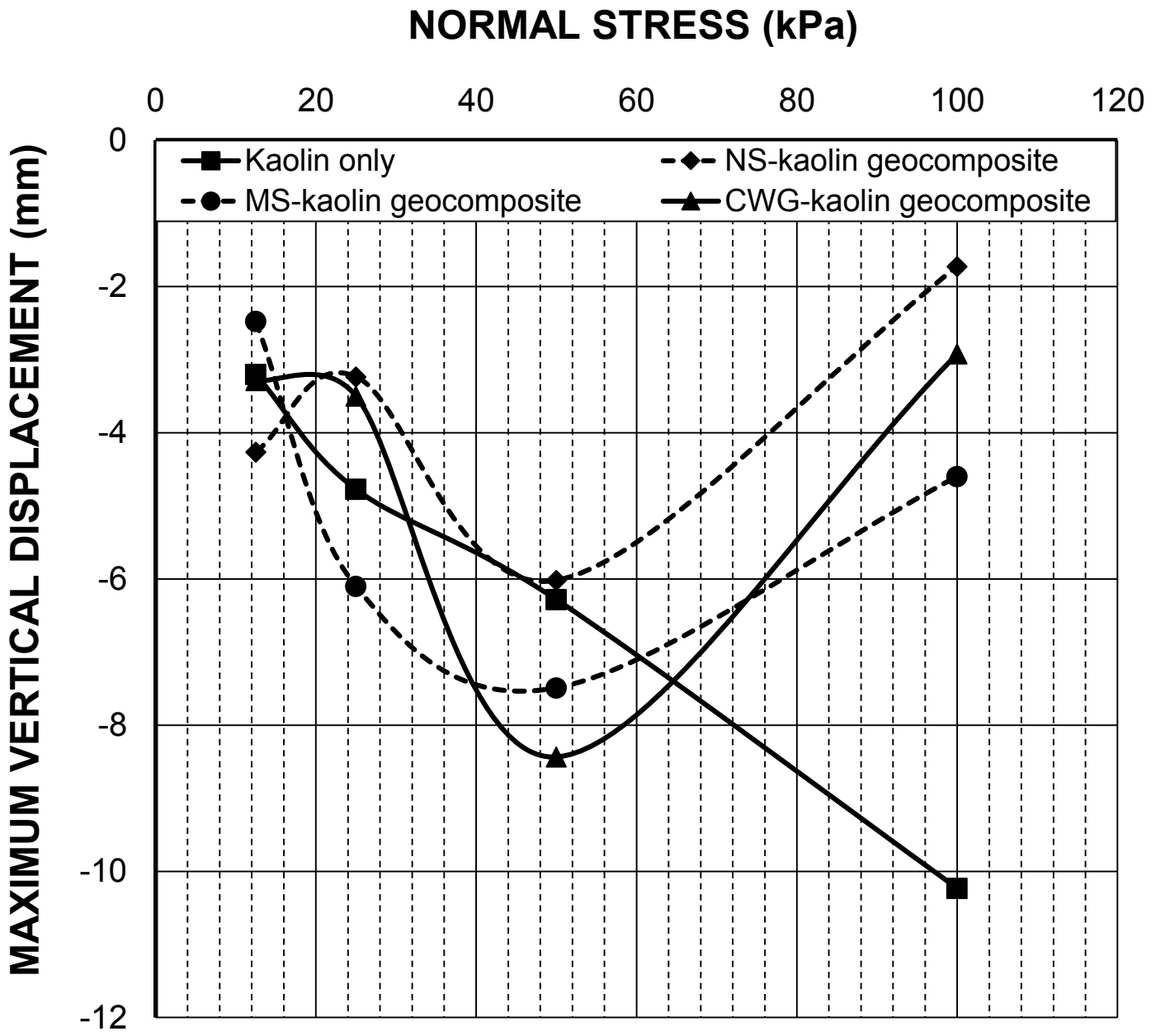

Figure 11